TAMPEREEN TEKNILLINEN YLIOPISTO
TAMPERE UNIVERSITY OF TECHNOLOGY

RIKU VIERIKKO

ELECTROMAGNETIC ISSUES IN AN ENGINE LABORATORY ENVIRONMENT

Master of Science Thesis

Examiner: D.Sc. (Tech.) Pertti Pakonen. Examiner and topic approved by the Faculty of Computing and Electrical Engineering on 31st. of May 2017

ABSTRACT

RIKU VIERIKKO: Electromagnetic issues in an engine laboratory environment
Tampere University of Technology
Master of Science Thesis, 60 pages, 2 Appendix pages
May 2017
Master's Degree Programme in Electrical engineering
Major: Power systems and -markets
Examiner: Pertti Pakonen, Project manager, D.Sc. (Tech.)

Keywords: Electromagnetism, disturbances, measurements, screening

The purpose of this study was to gather knowledge regarding electromagnetic emissions in an engine laboratory environment, to detect the sources of these and determine how to deal with the known disturbances that have been present in an engine laboratory. This was made by focusing first on the principles regarding the electromagnetic fields and methods how to avoid disturbances caused by them. At the end of the theory part this text will introduce occupational requirements for electromagnetic safety.

The study focuses on defining the electromagnetic fields in the engine laboratory by measuring emissions and electromagnetic fields generally with oscilloscope, spectrum analyzer and magnetic flux density meter. Measurements are meant to solve issues like: is the laboratory a safe working place in sense of electromagnetic fields, what kind of electromagnetic emissions are causing the disturbances, what is the source of the emissions?

The focus is on actions which are meant to reduce coupling of disturbances to signal conductors, and to analyze, how different actions are affecting propagation of emissions. This is done by testing a few of the presented procedures and measuring the emissions and the disturbances after these. The effects of the screening procedures are analyzed with tables, which are presenting numerical data on the effects of the screening. At the end, short conclusions regarding the results of the study will be drawn. Conclusions include also thoughts for further research regarding evaluation of the risks caused by electric- and magnetic fields in the laboratory environment.

TIIVISTELMÄ

Riku Vierikko: Sähkömagneettiset ongelmat moottorilaboratorioympäristössä
Tampereen teknillinen yliopisto
Diplomityö, 60 sivua, 2 liitesivua
Toukokuu 2017
Sähkötekniikan diplomi-insinöörin tutkinto-ohjelma
Pääaine: Sähköverkot ja -markkinat
Tarkastaja: Projektipäällikkö, tekn. tri. Pertti Pakonen

Avainsanat: Sähkömagnetismi, häiriöt, mittaus, häiriösuojaus

Työn tarkoitus on ollut kerätä tietoa moottorilaboratoriossa esiintyviin sähkömagneettisiin kenttiin liittyen, sekä selvittää niiden alkuperät ja tutkia miten välttää häiriöt joita on esiintynyt moottorilaboratorioympäristössä. Työssä keskitytään ensiksi sähkömagneettisten kenttien periaatteisiin ja menetelmiin, joilla sähkömagneettisilta häiriöiltä suojaudutaan. Teoriaosuuden lopuksi esitellään työterveyteen liittyviä terveysrajoja.

Tutkimus keskittyy mittamaan sähkömagneettisia kenttiä moottorilaboratoriossa oskilloskoopilla, spektrianalysaattorilla ja magneettivuon tiheysmittarilla. Mittausten tarkoituksena on selvittää: onko laboratorio sähkömagneettisessa mielessä turvallinen paikka työskennellä, minkälaiset sähkömagneettiset kentät aiheuttavat häiriöt ja mikä on häiriöiden lähde?

Työssä tutkitaan toimenpiteitä, joilla pystytään estämään häiriöiden kytkeytyminen signaalijohtimiin sekä analysoidaan miten erilaiset toimet vaikuttavat häiriöiden leviämiseen. Tämä on tehty testaamalla muutamaa esitettyä toimenpidettä sekä mittaamalla ympäristö näiden jälkeen. Tuloksia on analysoitu taulukoiden avulla, jotka esittävät numeerista dataa suojauksien vaikutuksista. Lopulta työn johtopäätökset esitellään lyhyesti. Johtopäätökset sisältävät myös ajatuksia jatkotutkimuskohteista liittyen sähkö ja magneettikenttien aiheuttamien riskien arviointiin laboratoriossa.

PREFACE

I wrote this thesis for Wärtsilä Marine Solutions. I want to thank Wärtsilä for this opportunity. Thanks to my thesis examiner Pertti Pakonen and Wärtsilä representative Sven Ingo. I also want to thank my friend Niko Polet, who gave enormous help to me regarding this study. Special thanks to my family and especially to my mother Riitta Vierikko, probably the bravest woman I know, and to my beloved girlfriend Outi Pohjavaara, who during the time I have been finishing this study gave birth to our little daughter.

Tampere, 19.5.2017

Riku Vierikko

CONTENTS

LIST OF FIGURES

LIST OF SYMBOLS AND ABBREVIATIONS

AC	alternating current
AL	action levels
C_c	coupling capacitance (F)
CISPR	International Special Committee on Radio Interference
D	distance (m)
d	diameter of the conductor (m)
DC	direct current
Diff	measured difference between the peak values measured when engine is running on 100 % load with and without steel bottom plates
E-Field	electric field
ELV	exposure limit values
EMC	electromagnetic compatibility
FFT	fast Fourier transform
H	strength of magnetic field (A/m)
HdB	strength of magnetic field in dB units (dBµA/m)
H-Field	magnetic field
HV	high voltage (U >35000V)
l	length (m)
f	frequency (Hz)
I_L	load current of radiating source (A)
I_1	fundamental frequency current (A)
$I_2, I_3, I_4, I_5 \dots I_n$	harmonic currents (A)
IARC	International Agency for Research on Cancer
ICNIRP	International Commission on Non-Ionizing Radiation Protection
IEC	International Electrotechnical Commission
LC-filter	filter which consists of inductance and capacitance
M	mutual inductance (H)
MV	medium voltage (1000 V<U<35000 V)
PEC	parallel earthing conductor
RMS	root mean square
t	time (s)
THD	total harmonic distortion (%)
U_1	fundamental frequency voltage (V)
$U_2, U_3, U_4, U_5 \dots U_n$	harmonic voltages (V)
V_L	voltage of radiating source (V)
Vn	induced voltage (V)
V_0	measured voltage induced by H- or E-field when engine is running on 0 % (1kW) load
V_{100}	measured voltage induced by H- or E-field when engine is running on 100 % load
V_{still}	measured voltage induced by H- or E-field when engine is standing still
V_{Screen}	measured voltage induced by H- or E-field when engine is running on 100 % load and the power cable ladders are screened by steel bottom plates
WDF	Wärtsilä dual fuel engine
WSG	Wärtsilä gas engine

W20	Wärtsilä engine type 20
Z_{in}	impedance between the reference point and the ground potential (Ω)
λ	wavelength (m)

1. INTRODUCTION

Nowadays transistor based applications have become common through processors, AC-drives, and power electronic applications. This has caused various electrical problems due to fast switching frequencies of these applications. Fast switching frequencies can create both magnetic and electric fields which may cause various of complex issues and errors. The source of these errors is usually difficult to detect making it difficult to block these errors from the system.

Wärtsilä has in their Vaasa engine laboratory numerous applications that use transistor based solutions, this leads to a need for this study. High frequency disturbances have been present inside their laboratory, which are likely caused by electromagnetic fields. The engine laboratory uses two types of generators as a load for the engines, external magnetized and a permanent magnet generator. The permanent magnet generator is connected through a converter to MV (medium voltage) system, where it is connected to the grid. In general, there are a lot of sensitive measurements taken around the engines. When the power is generated by the permanent magnet generator, a few of the measurements have been disturbed. These errors seem to be related to the permanent magnet generator, since disturbances are only present when generator is running. This leads to the question: what are the differences between the permanent magnet generator and external magnetized generator in sense of electromagnetic emissions.

The aim of this research is to gather the most important basics regarding electromagnetic fields, and to determine what is causing these errors in measuring circuits. The first goal of this study is to detect what causes these disturbances and what kind of electromagnetic emissions there are present around these generators. The second goal is to determine the differences between the external magnetized generator and the permanent magnet generator in terms of electromagnetic emissions. To ensure that there is no risk to health because of human exposure to electromagnetic fields, magnetic flux densities are measured from the test cells and places where people might be exposed to severe magnetic fields, and these results are compared to the limits set by the ministry of social affairs and health in Finland. In addition, the study is meant to provide knowledge regarding the electromagnetic relations and properties of electromagnetic fields and how to protect circuits from them. The references used in this thesis are technical literature mainly focusing on electromagnetism and how to prevent from harm caused by electromagnetic disturbances

To clarify the principles regarding electromagnetic compatibility the first section of the study focuses mostly to introduce the principles of electromagnetic emissions and protection against them. This is done by presenting the relations between emission sources and

the victims and by offering key principles regarding how installations should be done to offer the best protection against electromagnetic fields.

The second part of the text introduces the purpose of the study and conditions where these disturbances have been present. It gives specific information regarding the emission related equipment for giving the reader knowledge regarding the possible source of these emissions. It presents the disturbance records which were acquired to determine the properties of the emissions. It gives specific information how the disturbances have occurred and how they are measured and the setup of disturbance related equipment.

After this the study is focusing on measurements, which are meant to solve the source of the emissions and the behaviour of these emissions. It compares emissions originating from an external magnetized synchronous generator and a permanent magnet generator, that is connected through the converter to the grid. It presents the measurements and analyses whether the laboratory is a safe place to work in sense of electromagnetic fields.

At the end, this study introduces solutions how these emissions can be dealt with, and introduced solutions two screening actions are implemented. In the end this thesis gives an analysis regarding measurements after these actions. It also concludes whether the actions affected the errors and if they did, how? Finally, this thesis summarizes the study and presents proposals for further research.

2. ELECTROMAGNETIC EMISSIONS AND COMPATIBILITY

This chapter is focusing on presenting the principles regarding electromagnetic emissions and explains the relations between variables that are affecting coupling mechanisms. At the end of this chapter, a few generally used ways to avoid emission propagation and coupling of disturbances are presented.

2.1 Electromagnetic emissions

First of all, it is necessary to know what electromagnetic fields and waves mean and how they behave. This part of the chapter presents the basics regarding propagation of electromagnetic waves.

Potential difference between two separate nodes will form an electric field (E-Field) between them. E-field is measured in V/m units and is proportional to the voltage divided by the distance between these two nodes. When alternating current runs through conductor it creates magnetic field (H-field), which is measured in A/m units. When an alternating voltage creates an alternating current, an electromagnetic wave consisting of both E- and H-fields is created. The propagation velocity is determined by insulating material, while the properties of the radiating source determine both the wave strength and geometry of the field. The field may be dominated either by E- or H-field, depending on whether the dominant feature of the radiating circuit it is fast current oscillation or fast voltage oscillation. This depends on circuit impedance, a low impedance will create mostly H-field and high impedance will create mostly E-field. How these fields act, and what the distribution of these fields is depends on the physical properties of the source. The movement of these waves can be limited by the conductive screening [1, p.229].

Electromagnetic field can be divided into near field and far field depending on the distance from the source. The field at the distance of less than $\lambda/2\pi$ is called the near field, where λ is the electromagnetic wavelength which depends on radiation frequency. The wave length can be calculated by equation 1. In the equation f is the radiation frequency of electromagnetic wave, v is the velocity of wave propagation which is dependent of medium and λ is the wavelength. Properties of radiation source will determine the wave impedance in near field which is why the near field structure is relatively complex. In region of near field, it is necessary to consider E- and H fields separately. The radiating field at distances greater than $\lambda/2\pi$ or approximately 1/6 of the wavelength from the radiation source is called the far field. This means that both E and H fields are declining at the same ratio and therefore the wave impedance will stay constant. Radiating waves in

far field are known also as plane waves [1, p.229]. Because in far field the wave impedance stays constant, it is much easier to do the measurements and estimations for situations where the receiving object is located at far field region [1, p.225].

$$\lambda = \frac{V}{f} \qquad (1)$$

The propagation velocity of the wave will play a major role when defining the distance at which the electromagnetic field changes from near field to far field. For free space the velocity of propagation is the same as speed of light, which is 299 792 458 m/s [2, p.2]. This means that with a frequency of 100 kHz in a medium of free space, the transition from near field to far field happens at the distance of 477 m. In this case, it is unlikely that fields which cause the disturbances operate in far field distances, since potential emission sources in engine laboratory are not likely to cause severe emissions at frequencies higher than 477 kHz, which is the lowest frequency to create far field at distances below 100 m according to the equation 1. This is why this study focuses mainly on near field effects.

High frequency emissions that transistor based solutions like converters are supplying to their environment are composed of harmonics. Harmonics are caused by non-linear elements of the circuits, which leads that current that flows through these elements is not sinusoidal. Non-linear elements in this case mean transistor based switching devices like diodes or IGBT-modules. French mathematician Jean Baptiste Joseph Fourier discovered that a distorted waveform can be represented by sinewaves that are added to the base wave. Harmonic emission frequencies are dependent on the type of used rectifier. Typical 6 pulse rectifiers cause for example odd multiplier harmonics excluding the triplen harmonics, the harmonic component pattern is 5. 7. 11. 13. etc. The order of harmonic component is the multiplier by which the fundamental wave should be multiplied to get the frequency of that harmonic wave [18]. Triplen harmonics tend to sum at neutral conductor, which may cause difficulties, since neutral conductor may be sized smaller than phase conductors [23]. The total harmonic distortion (THD) is the sum of all harmonic components of the current or voltage waveform compared against to fundamental wave component of current or voltage wave. THD can be calculated for voltage with equation 2 presented below, where U_1 is the voltage of fundamental wave and $U_2, U_3, U_4, U_5 \dots U_n$ are voltages of the harmonic waves. This same equation can be used for calculating THD for current, by replacing U:s with I:s, where I_1 is fundamental wave current, and $I_2, I_3, I_4, I_5 \dots I_n$ are the current harmonic waves [27].

$$THD(\%) = \frac{\sqrt{U_2^2+U_3^2+U_4^2+U_5^2 \dots U_n^2}}{U_1} \times 100\ \% \qquad (2)$$

2.2 Conductive coupling

This part introduces principles regarding the conductive coupling, and introduces the two most common coupling mechanisms: common mode and differential mode coupling.

Conductive coupling mechanism means that emissions are coupled to victim equipment through direct electrical contact with a conducting body. Standards set by international special committee on radio frequencies (CISPR) have generally set the emission and immunity limits for the power supply because supply cabling is typically the main reason for emissions to spread or absorb. Emissions can absorb to the power cable through the equipment circuit or the power supply of the equipment. Emissions might also couple either capacitively or inductively from other cable to the supply cabling. [1, p.239]. However, compliance with the applicable standards does not necessarily ensure that the tested equipment is not involved in spreading harmful emissions to its operating environment. This is the reason why there might be a need to set even stricter emissions limits for certain operating conditions. Potential threats to cause conductive emissions are conductive transients, electrostatic discharges, supply voltage disturbances. These should all be taken in to account, if the equipment manufacturer wants to avoid considerable warranty expenses caused by conductive emissions [1, p.241].

For the understanding of electromagnetic fields related problems, it is vital to know the difference between the two most common conductive coupling modes: differential- and common mode coupling. Differential mode coupling consists of wires which have a connection to the same equipment e.g signal conductors. Because these wires have connection through the mutual impedance, the external field can couple with these conductors and generate emission currents to this loop. Earth reference is not involved in this kind of coupling [1, p.232]. A principle drawing of this coupling mode is presented in figure 1.

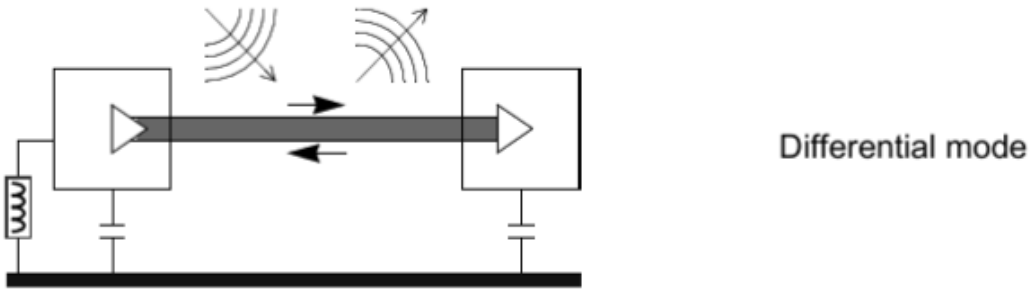

Figure 1. *Differential mode principle drawing [1, p.233].*

Common mode coupling consists of external or internal radiation coupled to the loop between the victim circuit and earth potential. Current flows in same the same direction through each wire. Loop is formed by various impedances that are connecting the victim circuit to earth potential, and allows the common mode current flow through the circuit

[1, p.232]. In case of common mode coupling, the most common emission absorbers are power transmission lines, cable screens, and other routes that allows current to flow for long distances and operate as large emission absorbing antennas [2, p.185]. In common mode coupling both the victim and emission source share the same earth potential, allowing emission currents to flow through the common impedance and this generates a voltage across the impedance of that loop. Common impedance can be in this case for example an open space between the two structures, which will couple structures through stray capacitances. The solution against this kind of emission spreading, is to isolate circuits electrically, which deletes the path of common current since coupling capacitance will not be present anymore [1, p.223]. Common mode coupling mechanism is presented in figure 2.

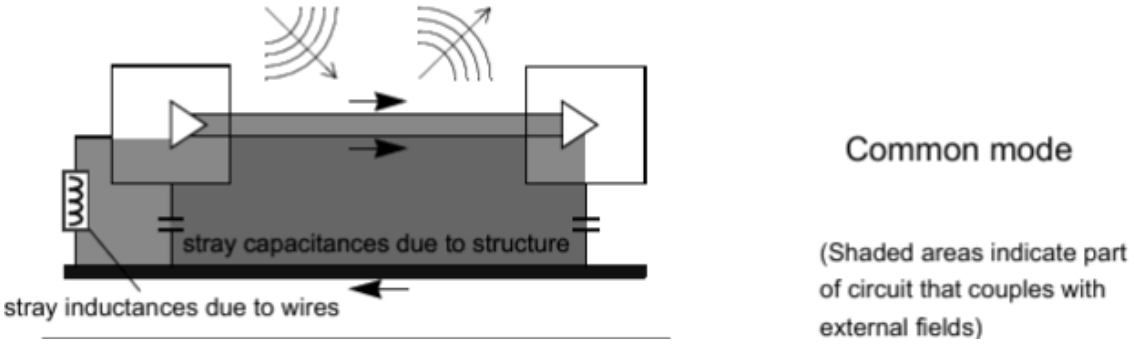

Figure 2. *Common mode coupling principle drawing [1, p.233].*

2.3 Magnetic and electrical induction

This part introduces some common emission coupling formulas, for situations where coupling occurs between two conductors spaced next to each other, like cables in tray installations are typically spaced. The intention of this is to show the principles how different variables affect coupling mechanisms and to give a basic understanding how to avoid harmful propagation of emissions by designing cable routes properly.

A H-field is generated when alternating current flows through a conductor. The H-field can induce a voltage to nearby conductors. This voltage follows equation 3 [1, p.224]. From equation 3 can be seen that the inducted voltage is proportional to mutual inductance M and rate of change of current I_L.

$$Vn = -M \times dI_L/dt \quad (3)$$

Mutual inductance M depends on: the diameters of the loops, the distance between the loops, orientation of the loops and the screening between the loops. The value of mutual inductance between cables which are spaced side by side for short distance can be in order of 0,1-3µH [1, p.224]. For example, when two cables are spaced next to each other and the length of the route that these are spaced to run in parallel is far longer than the distance

between these, mutual inductance can be calculated by using equation 4 [1, p.464]. In equation 4, l is the length of the route that cables are going side by side in meters and D is the distance between the cables in meters. The equation gives the result in Henry (H) units.

$$M = 0{,}2 \times l \times \left\{ \ln\left(\frac{2l}{D}\right) - 1 + \frac{D}{l} \right\} \times 10^{-6} \quad (4)$$

When a voltage is alternating in a conductor it creates an E-field. By capacitive coupling it induces voltage to conductors near it. Usually in cable installations the coupling capacitive reactance is far greater than the circuit impedances. In these cases, equation 5 can be used for defining the induced voltage [1, p.225]. Equation 5 is presenting that the main factors affecting to the coupling mechanism are coupling capacitance C_c, the rate of change of voltage V_L and the impedance to the ground of the victim circuit Z_{in}.

$$Vn = C_c \times \frac{dV_L}{dt} \times Z_{in} \quad (5)$$

Coupling capacitance C_c is determined by the distance between the two conductors, effective area and the screening of electrical field. In situations where two equally thick conductors are spaced next to each other with the medium of free space the coupling capacitance will follow equation 6, where l is the length that the conductors are running next to each other, D is the distance between the two conductors in meters and d is diameter of the conductors in meters. [1, p.463]. Equation 6 gives the result for coupling capacitance in Faraday (F) units.

$$C_c = \frac{\pi \times 8{,}85 \times 10^{-12}}{\cosh^{-1}\left(\frac{D}{d}\right)} \times l \quad (6)$$

The similarity between these two effects is, that both are generated by alternating current or voltage. Equations 4 and 6 are presenting that both mutual inductance and coupling capacitance are proportional to the distance between the victim and source conductors and the length of these cables run in parallel. If either one of these distances is increased, it will decrease the values of mutual inductance and coupling capacitance, which means that also the induced voltages will be decreased. Figure 3 presents the effects of separation distance on the coupling capacitance and mutual inductance. It confirms that greater separation distance will reduce coupling factors, so it is easy to draw conclusion that spacing is crucial factor to avoid defects caused by radiating emissions between the cabling [1, p.226].

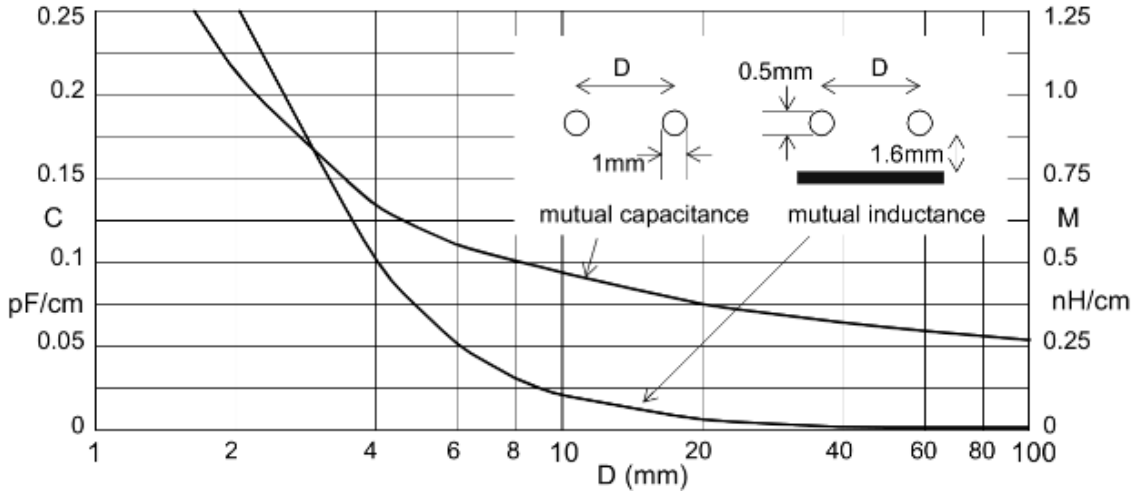

Figure 3. *Effects of cable separation distance to mutual coupling factors [1, p.226].*

2.4 Electromagnetic fields and human health

There is no clear scientific proof that H-fields are a health risk, however many researches have gathered statistical data indicating that living in regions where transmission lines are causing a H-field which magnetic flux density is 0.4 µT or higher, doubles the risk of children to get leukaemia. Because of this the International Agency of Research on Cancer (IARC) has classified low frequency H-fields as a phenomenon which "possibly causes cancer". Risks seems to be limited only to low frequency H-fields. There is no statistical data indicating that E-fields are causing health risk to human health [14]. However, docent of medical science Leena Korpinen has gathered a table on her internet pages which presents that a low frequency E-field exceeding the 70 kV/m or a low frequency H-field exceeding 4 mT, can cause flashes (fosfens) to human vision. It also shows that low frequency E-field exceeding the value of 7000 kV/m or low frequency H-field exceeding the value of 100 mT might cause ventricular fibrillation to the heart [4].

The Ministry of Social Affairs and Health has set maximum exposure limits for the E- and H-fields radiation to the law of occupational health and safety, which determines exposure limits to conditions where workers might be at risk of electromagnetic fields [17]. The Ministry of Social Affairs and Health has set also the recommendation limits for continuous magnetic and electric radiation for public exposure [15]. Limits for occupational health and safety are generally higher than the limits for public exposure since occupational exposure will last about 8 hours and public exposure might in theory last for up to 24 hours in a day [25]. Tables 1 and 2 are presenting occupational health requirements by action levels (AL). How employer should proceed in situations where these limits are exceeded is guided in directive 2013/35/EU. In general, ALs can be exceeded if employer proceeds certain pre-cautions only if the H- or E-fields do not exceed the exposure limit values (ELV) [17]. These limits do not ensure that electromagnetic fields will not cause dysfunction for electrical equipment which are used for body functions

such as pace maker. However, most pace makers are working properly in magnetic flux density up to 0.5 mT [15].

Table 1. *H-field occupational health and safety requirements in EU [26].*

Frequency range	Magnetic flux density Low ALs(B)[μT] (RMS)	Magnetic flux density High ALs(B) [μT] (RMS)	Magnetic flux density ALs for exposure of limbs to a localised magnetic field [μT] (RMS)
1 ≤ f < 8 Hz	$2{,}0 \times 10^5/f^2$	$3{,}0 \times 10^5/f$	$9{,}0 \times 10^5/f$
8 ≤ f < 25 Hz	$2{,}5 \times 10^4/f$	$3{,}0 \times 10^5/f$	$9{,}0 \times 10^5/f$
25 ≤ f < 300 Hz	$1{,}0 \times 10^3$	$3{,}0 \times 10^5/f$	$9{,}0 \times 10^5/f$
300 Hz ≤ f < 3 kHz	$3{,}0 \times 10^5/f$	$3{,}0 \times 10^5/f$	$9{,}0 \times 10^5/f$
3 kHz ≤ f ≤ 10 MHz	$1{,}0 \times 10^2$	$1{,}0 \times 10^2$	$3{,}0 \times 10^2$

Table 2. *E-field occupational health and safety requirements in EU [26].*

Frequency range	Electric field strength Low ALs (E)[Vm^{-1}] (RMS)	Electric field strength High ALs (E) [Vm^{-1}] (RMS)
1 ≤ f < 25 Hz	$2{,}0 \times 10^4$	$2{,}0 \times 10^4$
25 ≤ f < 50 Hz	$5{,}0 \times 10^5/f$	$2{,}0 \times 10^4$
50 Hz ≤ f < 1,64 kHz	$5{,}0 \times 10^5/f$	$1{,}0 \times 10^6/f$
1,64 ≤ f < 3 kHz	$5{,}0 \times 10^5/f$	$6{,}1 \times 10^2$
3 kHz ≤ f ≤ 10 MHz	$1{,}7 \times 10^2$	$6{,}1 \times 10^2$

2.5 Ways to provide EMC in cable installations

External cabling is known to be a common source of radiating emissions. This part introduces applicable solutions for preventing disturbances to couple or to propagate from the cable installations. It also introduces the ways to ensure proper performance of screening.

In cable installations, differential mode currents flow through one wire in one direction and through another wire in the reverse direction. These currents tend to be equal. The loop area formed by these conductors is relatively small and the currents tend to cancel each other, making the net radiation caused by differential currents usually low. A cable screen is not normally involved in this type of radiation propagation [1, p.340]. Common mode currents will flow all in the same direction, which means that they will create their own H-field. This is where the cable screen might be part of, and this must be considered when screening is designed. Common mode coupling is a coupling method also known as longitudinal conversion loss. It happens when the conductor has a potential difference

against earth and is coupled through the stray capacitances to the earth. This creates relatively big current loop, which means that even low common mode current can generate significant magnetic fields [1, p.340-341]. Induced high frequency currents will be separated to the outer and inner surface of conductor because of the skin effect. The H-field caused by these screen currents can be blocked by using a braided screen cable. It is a cable where braid strands are continuously woven from the inside to the outside and back again. This waving aims to minimize the H-field caused by skin effect currents [1, p.347].

All return wires are preferred to run as near as possible to their supply wires since this minimizes coupling of external H-fields. The reason for this is that H-fields formed by supply and return wires tend to be exactly the same, but in opposite directions. Leading to the H-fields cancelling each other out. In theory if cables are installed to run exactly the same route, the inductance of loop formed by supply and return wires should be zero, meaning that the loop does not receive any energy from the external H-fields. In practice this is impossible, but this operation principle is used in solutions like twisted pair and coaxial cable. Both solutions are used for reducing the loop reactance and reduce H-field coupling [1, p.341]. This is the reason why properly made spacing reduces the H-fields coupled with the cabling. This same principle is applicable to circuits that might cause H-fields i.e. power cabling. The reason for this is that, when supply and return cables are spaced very close to each, they will form low inductance. Since inductance is the key factor in generating H-fields it will reduce the H-fields originating from the cabling [5, p.179].

In power cable installations twisted pair have not been used as solution since the size of the used cables. For power cables the best option for installation to get maximum EMC advantages is to install all cables side by side and space as close to each other as possible. However this might cause too powerful magnetic forces which might damage the insulation of the cables, which is why cables might have to be installed with greater separation distances at the expense of electromagnetic protection. This kind of solution is where extra separation distances should be applied for the sensitive equipment [5, p.188].

Screening can be used to prevent cables from coupling electromagnetic emissions to environment. It can be used also to prevent cable from create unwanted electromagnetic fields to its environment. In cable installations done by using screened non-twisted pair cable, if the screen is connected only on one side to earth, screening provides good protection against E-fields, but does not provide protection against H-fields. This is shown in figure 4 picture a). For protection against the H-fields, cable should be connected from both ends to the ground potential. This practice allows induced current to discharge to the circuit formed by the screen and ground potential, and by this way prevent the centre conductor from coupling with external H-fields. Figure 4 picture b) presents this operation principle. The protective functionality of the screen will reduce the coupling of radi-

ation after the emission frequency reaches the cut off frequency of a cable. Cut off frequency is a cable specific value usually given by the cable manufacturer. It can be for braided screen around 1-2 kHz and for aluminium foil around 7-10 kHz. After the emission frequency reaches the value of 5x cut off frequency, the induced voltage at the centre conductor will stay constant [1, p.344]. Figure 4, picture c) introduces the behaviour of screening effectiveness in a function of frequency. Under the plot is presented an equation, which determines the cut off frequency, where Rs is the resistance of the screen and Ls is the inductance of the screen.

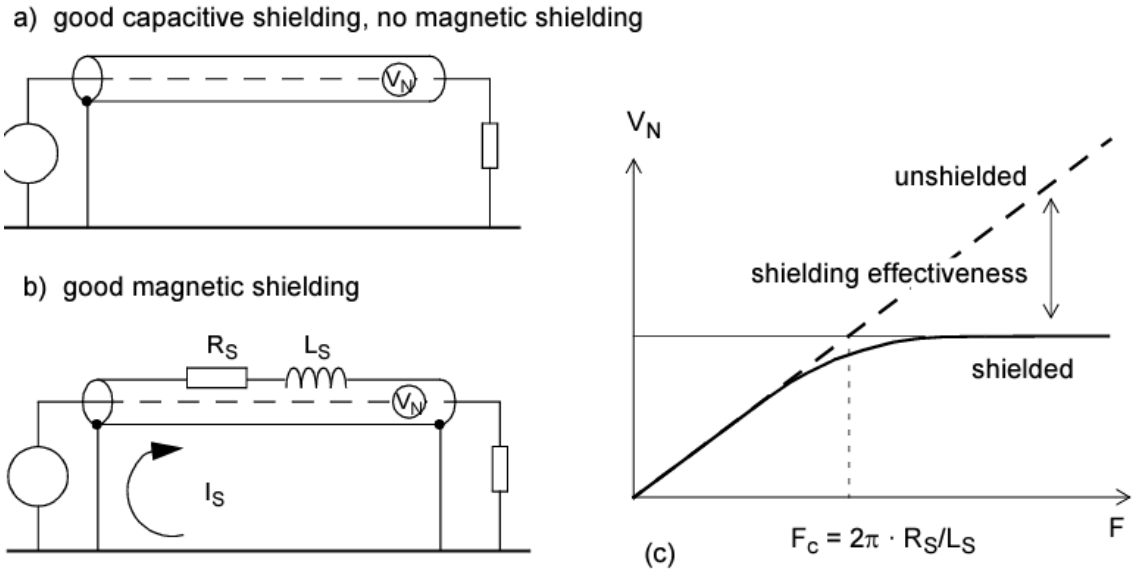

Figure 4. *Properties of cable screen [1, p.345].*

When screened cable is used in cable installations, it is important to make sure that the screening circuit has as low impedance as possible. This can be done by ensuring that the screen connection is done properly straight to the metallic mounting plate or -frame. The best way to do this is by connecting the screen by 360-degree connection straight to the frame. Figure 5 introduces a couple of commonly used screen connection methods, clamp, gland, and the pigtail connection. The most convenient connection type for this is a connection with a conductive cable gland, a well-made conductive clamp connection to mounting plate is also an acceptable alternative. When a clamp connection is used the mounting plate surface must be either coated or made from a conductive material and the conductive connection between the mounting plate and panel frame must be ensured, otherwise protection will not work properly [1, p.349]. The connection type in which the cable screen is gathered to a single wire and this “tail” is connected through the terminal to the earth potential is called a pigtail connection. It is a commonly used connection type because it is easy to build, and some older data sockets will only offer this type of connection. However, this is not a good method in sense of electromagnetic protection. At high emission frequencies it might even be as bad way of connection as no connection at all. This is because of inductance that pigtail loop forms, might cause its own H-field, this

might couple with the signal conductor. In cases where pigtail connection is the only way to do earth connection, the tail should be as short as possible and preferably done with two or more connection points. These points should be located in opposite directions of each other to minimize the inductance that is caused by the pig tail [1, p.351]. Figure 5 presents these three common screen connections.

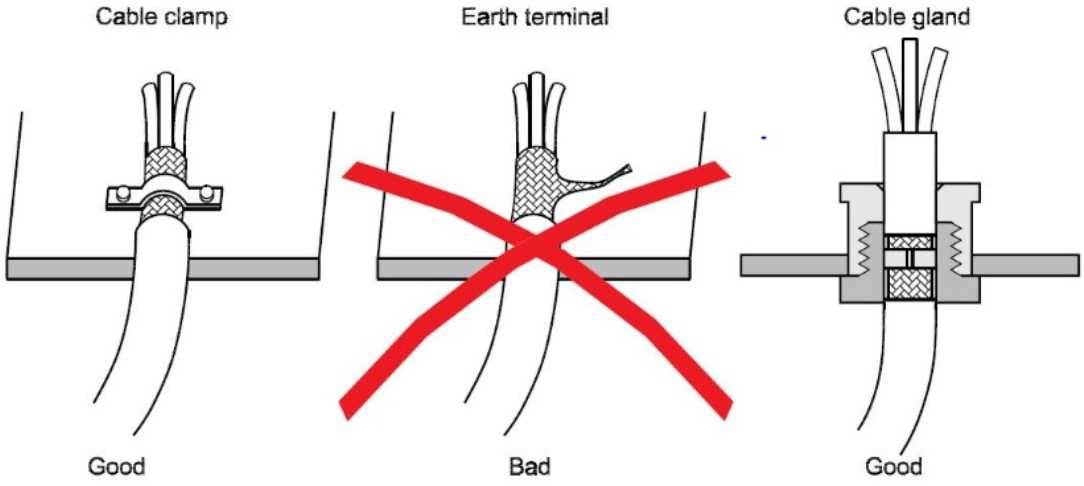

Figure 5. *Common screen connections [11].*

It is important to notice that conductive cable screening works only for frequencies above the cut off frequency. There is no effective way for protection against H-field coupling at low emission frequencies only by using conductive screening. [1, p.344]. Protection to prevent from H-field emissions caused by frequencies below the cut off frequency can be made by using a high permeability screen, like mu-metal. When a high permeability material is used, it is important to make sure that the flux density does not exceed the saturation density of the high permeability material used, since if the density exceeds the saturation density it will start to saturate the high permeability material. The permeability of these high-mu materials tends to regress when the emission frequency rises above a couple of kHz [1, p.384]. As an alternative solution against the coupling of low frequency H-field is increasing the separation distance between the radiation source and the victim. This lowers their mutual inductance reducing the H-field coupling between them [1, p.226]. H-fields caused by high currents can be reduced effectively by spacing power conductors to run as a bundle or laid side by side as close as possible [5, p.188]. If there is need for protection also against higher frequencies, the applicable solution would be a combination of both high-mu screening for low frequency magnetic emissions and conductive material screening for both E-field and high frequency H-field emissions [1, p.384].

As it was mentioned earlier, cable routing can be used to avoid the electromagnetic propagation. For this reason, cabling is classified in T. William´s and K. Amstrong´s book,

EMC for Systems and installations by 6 different cable classes depending on, how sensitive or noisy certain type of cabling is assumed to be. This classification suggests the minimum physical separation distances between the different cable classes and specific installation instructions for each [5, p. 180]. These are presented below

Class 1 is for very sensitive signals, commonly applied for cables that contains low level signals like measurement signals and high speed digital signals like Ethernet and video signals. General rule is that if signals are operating with less than 1 V voltage or 1 mA current, the source has an impedance higher than 1 kΩ or the operating frequency is higher than 1 MHz, the cable is classified as class 1. Class 1 cables should always be high quality twisted pair cables with 360-degree continuous screen [5, p.180].

Class 2 is for quite sensitive signals, which include basic analogue signals like 4-20 mA and 0-10 V for frequency under 1 MHz and low speed digital/bus protocol like RS232, RS422, RS485 and Entronics. It also includes digital inputs and outputs like signals from limit switches and encoders. Applications where classification 2 cables are, it is recommended to use screened cables in installations [5, p.180].

Class 3 is for bit disturbing signals includes external AC (alternating current) supply up to 230/415V or DC (direct current) power supplies which do not supply any external noisy equipment like converters, welding machines etc. External equipment must be considered noisy, if there is no information available on whether the equipment fulfils the harmonized EMC emission standards. Fulfilling these standards usually requires internal supply filters. Class 3 also covers control circuits with resistive or/and inductive load, like coils of solenoids and contactors which inductive loads are fitted with filters. Cabling to an induction motor belongs to class 3 if the motor is controlled by an on/off type switch or speed controlled by a converter which has sinusoidal output filters. Cabling for class 3 can be done by using screened cables, multiconductor cables or even single wires. However twisted pairs are always preferred [5, p.180].

Class 4 cabling is for heavy disturbing signals includes cables that are connected to power inputs or outputs, or DC-links to speed adjustable motor drives, welding machines and all the similar noisy equipment. Converter type equipment can be considered noisy if there is suspicion that any of the power in-/output are unfiltered. Cables for on/off controlled DC motors and slip ring motors are also considered to be class 4 although sparkles DC motors or motors with inner filters can be considered as class 3. In addition, class 4 includes unsuppressed control cabling to inductive loads and all cables to radio transmitting antennas. Cabling for class 4 should be done with high quality braided screen cables. Screen of the cable must be connected via properly made connections to earth, pigtails are not acceptable [5, p.181].

Class 5 cabling consists of medium voltage (MV) –cabling and class 6 consists of high voltage (HV) cabling. These both are exposed to external disturbances like lightning

strikes and surges which are caused by fast operations of breakers. Cabling and installations are usually designed by power engineers [5, p.181].

The recommended separation distances between the cable classes are presented in figure 6. It presents, the suggested minimum distances between the cable classes for runs of up to 30 meters when cables are spaced in parallel close to parallel earthing conductors (PEC). For longer runs distance should be multiplied by l/30, where l is length of the run in meters. Separation between class 5 and 4 should be 150 mm at minimum and distance between 1 and 5 should be at least 750 mm. Class 6 cables should be separated from class 4 with at least 150 mm. Class 1 cabling should be protected with metal conduit if it is routed closer than 1 m distance from class 5 or 6 cables class [5, p.182].

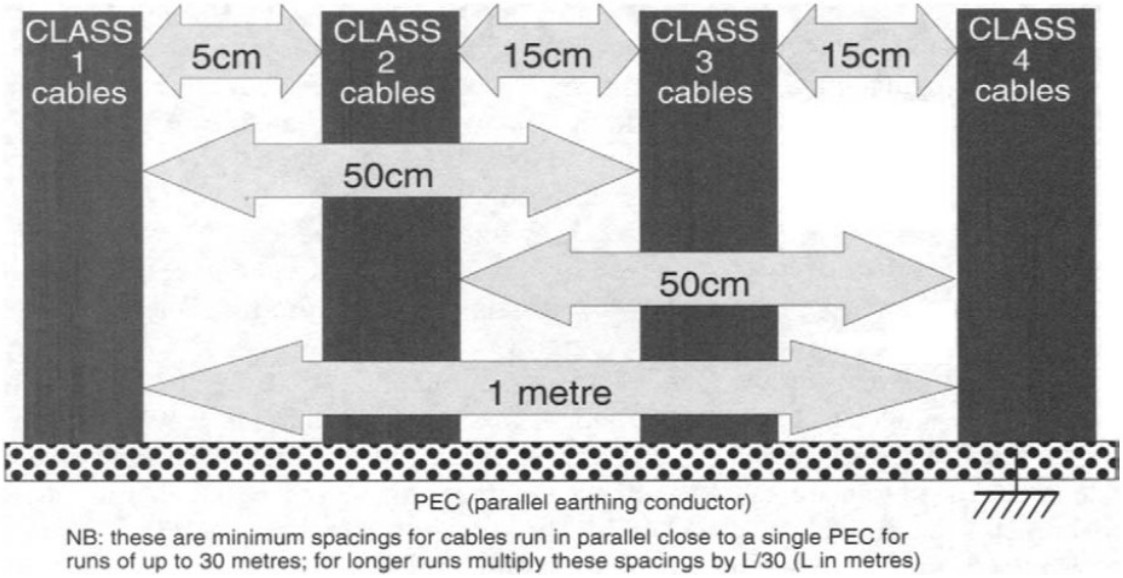

Figure 6. *Minimum separation distances [5, p. 184].*

For cable installations PEC (Parallel Earthing Conductor) can be used to provide extra screening against electromagnetic emissions. The main task of PEC's is to take off heavy earth currents for both the cables and the cable screens. Since earth currents are usually 50 Hz and energy caused by lightning surges are mostly below 10 kHz frequency, the requirements for PEC is just to provide low resistance and high current withstand. Typical cable support structures have sufficient cross sectional area for using as PEC. Even cable armour can be used as PEC, if it is connected to earth potential form both ends. In this case, it is necessary to ensure that there are no breaks in the PEC loop. PEC can reduce the high frequency emission absorption by its screening performance, and cable ladders are not as effective for this purpose as for example a metal conduit would be. Cables should be installed as near to their PEC as possible to prevent from magnetic coupling caused by circulating currents between PEC and cable conductors. Figure 7 below illus-

trates suitable PEC structures to protection against high frequency electromagnetic emissions, the PEC:s are presented in order from worst to best in terms of PEC:s EMC properties, where number 1 means the worst and number 7 means the best [5, p.188].

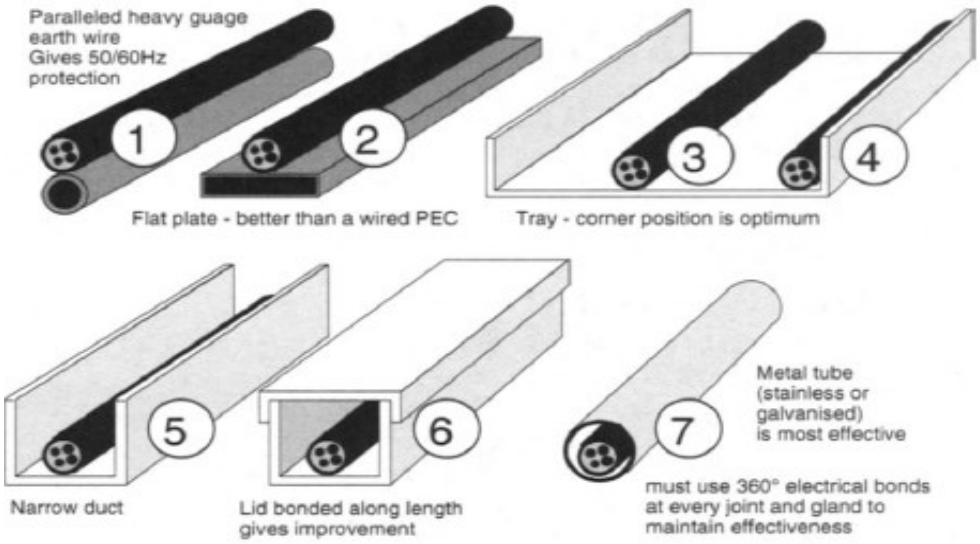

Figure 7. *PEC:s shorted by screening properties [5, p.189].*

2.6 Filtering the emissions by low pass filter

Filtering is solution for attenuating propagation of emissions caused by high switching frequencies. It is used to prevent emissions to propagate either in or out from the equipment interfaces. This reduces conductive emissions directly and radiating emissions if the cabling is the source causing the radiation. This part introduces principles regarding the filtering of emission frequencies.

In a typical situation emissions that are connecting through the interfaces have a higher frequency than the wanted signals. This makes emissions easy to attenuate with a low pass filter. Of course, this is not the case always, since there are for example, wide band signals where wanted signals might operate at higher frequencies than emissions. A typical low-pass filter consists of serial connected inductance or resistance and parallel connected capacitor. An inductance can offer higher resistance for radio frequencies with less low frequency power loss compared to resistance. A resistance however will not cause resonance situations and it is usually cheaper alternative for series component. Capacitors provide low impedance for high frequencies and by this way they will attenuate emission frequencies. They operate in the best way possible when they are connected to a high impedance circuit, which is the reason why usually either a series resistance or a series inductance is used in the same circuit with the capacitors [5, p.193]. Figure 8 presents a typical function curve of a single stage low-pass filter, it shows that this filter starts to

attenuate after the frequency passes the cut-off frequency and the filtering is more effective with increasing frequency. The cut off frequency of this particular filter is at the frequency of 1 kHz.

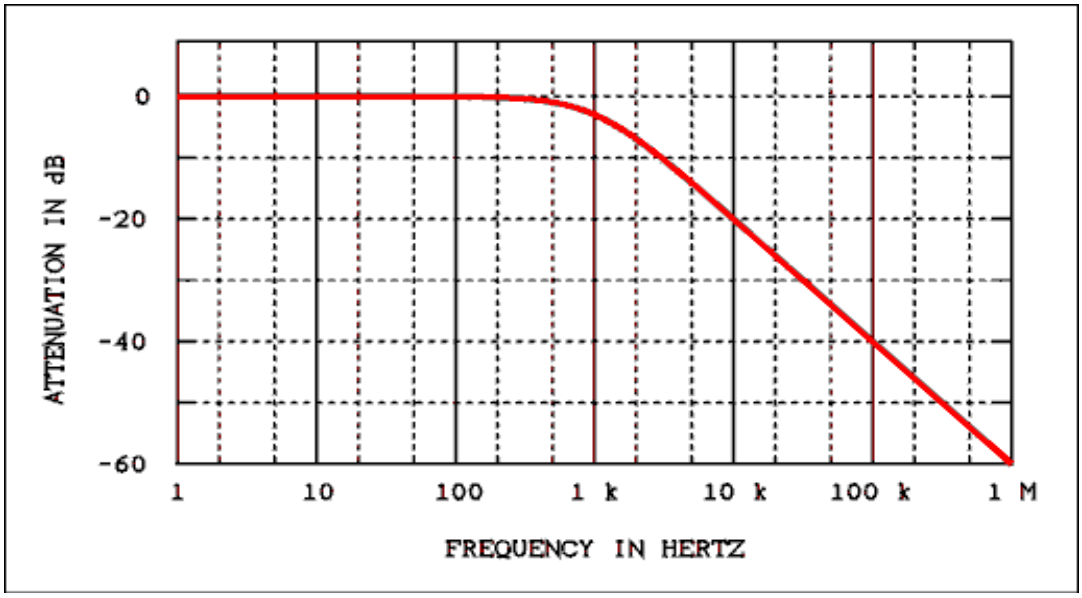

Figure 8. *Attenuation of single stage low pass filter as a function of frequency [13].*

A filter is designed in a different way depending on whether it is meant to prevent from common mode or differential mode coupling. This is because a common mode filter does not work properly against differential mode emissions and differential mode filter does not work against the common mode emissions. Figure 9 presents how the implementation of filtering differs between these two coupling modes [5, p.194]. However, it is possible to implement these both methods in same filter, which is commonly used solution for mains filtering [5, p.201].

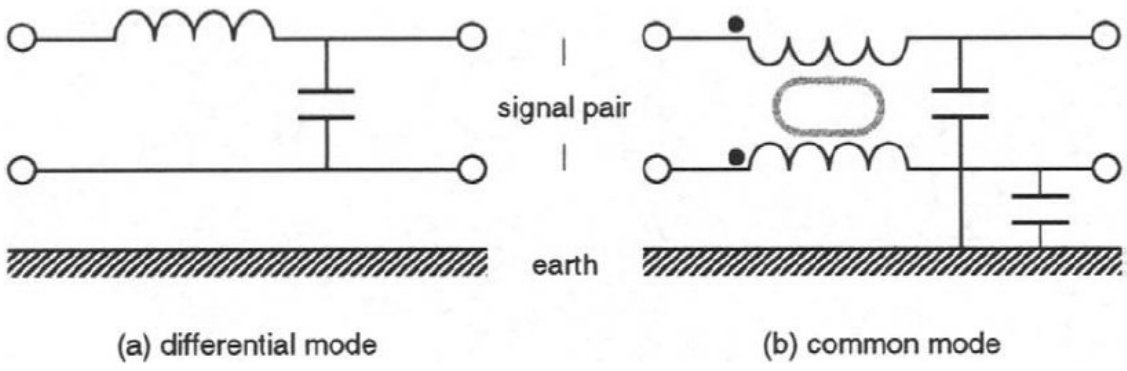

Figure 9. *Common- and differential mode filtering [5, p.194].*

In most cases the performance of a filter is presented as performance with 50 ohm source and load impedances, which is done in accordance with standard CISPR 17 – Methods of measurement of suppression characteristics of passive EMC filtering devices. Filters do

not actually operate in this kind of circuit, because these impedances are usually both frequency and time dependent. For example the source impedance might vary in range of 2 ohms to 2000 ohms. This can become a problem since performance of the filtering strongly depends of the impedance which is present at the terminals [5, p.195]. This is why some suppliers are nowadays offering information regarding attenuation performance with 0.1 ohm/100 ohm, and 100 ohm/ 0.1 ohm source and load impedances, which is meant to facilitate the evaluation with differing characteristics of source and load impedance.

Filters which are manufactured from inductances and capacitors (LC-filter) are resonance circuits. This means that if a circuit that is filtered with an LC-filter contains emission frequencies that are in resonance range, then instead of attenuating the filter starts to amplify the emissions at this specific frequency range. This leads to a situation where filter might increase the emissions instead of attenuating them. This issue can be fixed by usage of two- or multi stage filters, which are not as dependent on the source/load impedances [5, p.196]. A typical mains filter will provide both common- and differential mode filtering. Figure 10 presents a typical construction of a mains filter [5, p.201]. It is a passive component, meaning that it does not matter which terminals are used for supply or load terminals, only terminal pair must be connected correctly [5, p.202].

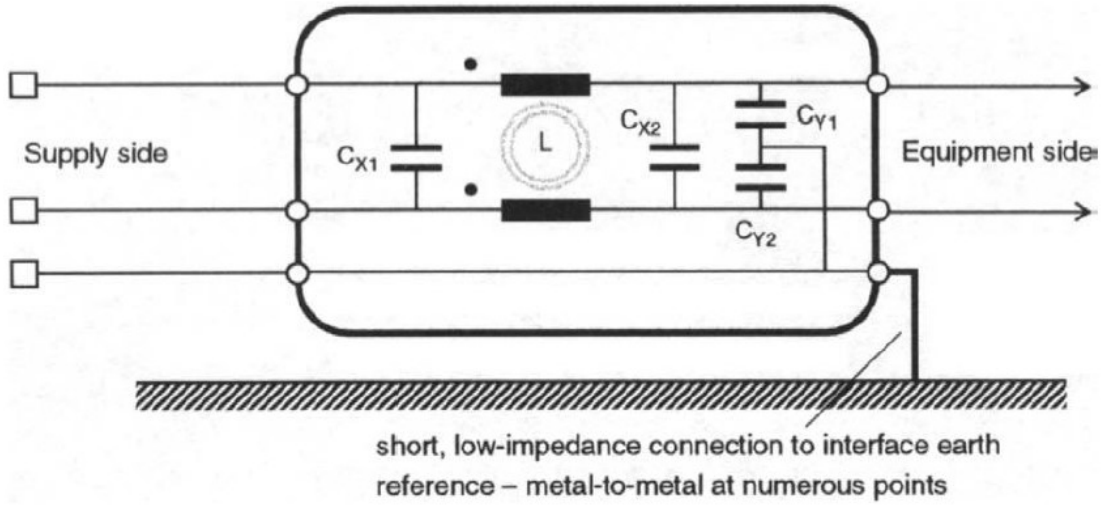

Figure 10. *Structure of a typical mains filter [5, p.201].*

2.7 Measuring the electromagnetic emissions

The following part will introduce some key principles regarding electromagnetic measurements. Traditional measuring techniques are partially useless for the purposes of this study because high frequency radiated emissions reach up to 1 GHz. This part introduces a measuring receiver, a spectrum analyser and a tracking generator and transducers that are used for measuring with them. It also introduces Hioki magnetic flux density meter

since it is used for measuring for occupational health and safety requirements further in this study.

Commercial standards like CISPR have drawn the border line between conducted emissions and radiated emissions at the frequency of 30 MHz. This means that most of the standards have not set radiated emissions limits for frequencies below 30 MHz. They also have not defined conducted emission limits for frequencies above 30 MHz [1, p.234]. In reality an exact borderline at 30MHz does not exist and it is in fact quite common to have radiated emissions that have a frequency below 30 MHz. Even succeeding in compliance measurements, does not necessarily mean that equipment will not cause any harmful radiating emissions to its operating environment. There are generally three different kind of measurement devices that are used for EMC-compliance measurements. These devices are the measuring receiver, the spectrum analyser and the tracking generator [1, p.118].

A measuring receiver is used usually when the aim of the measurement is to do standard based compliance measurements. This is because it usually offers more accurate measurements than a spectrum analyser, although some spectrum analysers can be just as accurate. A measuring receiver is usually expensive compared to spectrum analyser, but it has the advantage of offering better sensitivity and higher dynamic range, by allowing signals to be discriminated from the noise at very low levels. It also generally offers a better frequency and amplitude accuracy and it can handle overloads better than a basic spectrum analyser [1, p.118].

A spectrum analyser is usually a lower price alternative to a measuring receiver, and its main purpose is doing “quick check” testing and disturbance diagnostics. A basic spectrum analyser is not able to offer the same sensitivity as the measuring receiver. It has less dynamic range, which means that wideband signals with high contained energy might cause saturation and therefore the spectrum analyser might start to give erroneous measurement results. It is sensitive to the overloads, because overloads can damage the mixer diode of a spectrum analyser. An overload can be a quick transient or constant overload in input. A spectrum analyser can be upgraded by installing a pre-selector that provides similar performance to a spectrum analyser as a measuring receiver has. Pre-selector is a separate unit which consists of input protection, an input amplifier and a sweep adjusted filter. It is locked to the spectrum analysers input. In practice, it increases the accuracy and dynamic range of the measuring device and protects the spectrum analyser from overloads. As a disadvantage, pre-selector costs nearly as much as spectrum analyser almost doubling the total cost of the measuring device [1, p.119].

A tracking generator is a signal generator which is used in co-operation with a spectrum analyser or measuring receiver. It is used for simulating disturbances to the network or system, the output of which is connected to the spectrum analysers input. With the use of a tracking generator, it is possible to characterize the radio frequency losses from the cables and sum attenuation of a system. In general tracking generator is used to test the

following properties of the tested system: filtering, attenuation, amplifying and screening properties of enclosures or cabinets. Properties which are essential for system characterization and product development [1, p.121].

A transducer is required for connecting any high frequency emission to a measuring device. There are different types of transducers for measuring each of the following: E-fields, H-fields, conducted voltage and -current emissions. In this context, an antenna is a transducer as well because it is used for measuring the radiated emissions. In measurements where an antenna is required, it must be oriented as it gives maximum response and it is necessary to know the antenna factor of used antenna. The antenna factor basically informs how the antenna converts the electromagnetic field into voltage at its terminals at each frequency. It is added to the measured voltage to obtain the E- or H-field strength. To get accurate measurements both the antenna factor and cable attenuation must be counted together with the measurement result. The antenna factor is typically given by the manufacturer for each wide band antenna in a table, where frequency specific antenna factors are presented by dB/m- units [1, p.126].

A loop type antenna is used for measuring the H-field at frequencies below 30 MHz. The loop is like a coil that generates a voltage proportional to magnetic flux and frequency in accordance with faradays law. A low impedance loop itself is not suitable for a 50 ohm testing input, but it can be fixed with preamplifier. A preamplifier can fix the impedance of a loop probe to a value of 50 ohms resulting a flat antenna factor, making measurements equally accurate throughout the entire frequency region [1, p.130].

A monopole antenna is used for measuring the E-field typically up to 30 MHz frequency. It is a single vertical rod, which is located approximately 1 m above the reference potential or earth plane and is used to measure E-field in vertical polarization. A monopole is short in electrical manner, which means that its length is much less than wave length. It has capacitance of few pF, so it has to be connected to measuring equipment through a high impedance preamplifier to maintain the impedance of 50 ohm. This practice ensures that the antenna factor is constant at all frequencies. Combination is sensitive for external E-fields so it needs an overload indicator and high-pass filter to neutralize the effects of the mains field. Because of E-Field is affected by near conductive structures, accuracy and repeatability of test is not very good [1, p.130].

Real time spectrum analysing is a technology, that allows measurements from the spectrum in real time. Its performance of is based on fast fourrier transform technology (FFT) without leaving any gaps working in real time. The real time spectrum analyser is designed to capture all events that occur in a frequency spectrum for specific bandwidth. It possesses more extensive triggering capability, which allows to trigger on specific events in the frequency domain, not just power or external triggers. A real time spectrum analyser provides more specific information regarding the transient signals than a traditional swept time spectrum analyser provides [19].

For the conformance of environmental exposure limits there are specific meters, that are meant for measuring radiation exposure in environment. One example of these is Hioki FT 3470, which measures magnetic flux density. It is designed to measure in conformance of standards like International commission on non-ionizing radiation protection guidelines set in 1998 (ICNIRP 1998) and IEC62233 standard Measurement methods for electromagnetic fields of household appliances and similar apparatus with regarding human exposure. These guidelines set the limits of human exposure to magnetic radiation. Hioki 3470 offers automatic exposure level measurements, which means that it can calculate percentage automatically from healthy requirements set by ICNIRP 1998 [20]. Occupational exposure measurements are no longer valid in Finland, since the limits have at 2016 been re-adjusted and are now nearly two times higher. For example at the ICNIPR 1998 limit for 50 Hz magnetic flux density was set at the value of 500 µT, which is at the latest ICNIRP 2010 and the occupational health and safety requirements set by Finnish health department set to value of 1000 µT [24] [25]. Besides exposure measurements Hioki provides magnetic flux density measurements for frequency ranges of 10 Hz-2 kHz, 2 kHz-400 kHz and 10 Hz-400 kHz. It can measure the sum H-field from three dimensions and calculate the magnetic flux density from this measurement [20].

3. DISTURBANCES IN ENGINE LABORATORY MEASUREMENTS

This chapter presents the engine laboratory and the equipment that have been involved in electromagnetic disturbances. The aim of this is to describe the study more specifically by presenting working environment and the components that might be involved in these disturbances. It also presents a setup where the disturbances have been present and the disturbance records. Presenting these disturbances eases the way to analyse propagation of electromagnetic radiation and might make for reader easier to understand the purpose of this thesis.

3.1 Wärtsilä engine laboratory and test cell 3

Wärtsilä has an engine laboratory in Vaasa city including 4 test cells that are used for testing engines. These tests are generally aiming to test engine performance and durability. Wärtsilä uses generators for loading the engines. The generators can generate power either to the grid or to the load resistors. Generators are generating notable power, which means that sensitive equipment are constantly exposed to electromagnetic emissions caused by power system. Electromagnetic disturbances have been observed in test cell 3 for which this part gives a short presentation.

Test cell 3 has an engine type WDF under the test, which can run on heavy fuel oil, light fuel oil and natural gas. The engine is loaded via a permanent magnet generator which differs from other engine generator sets used in engine laboratory environment, which are using external magnetized generators as a load. The output power of the generator is supplied to the grid through a power converter. Power is generated at various speed and load. The engine has a nominal speed of 750 rpm and a nominal power of 5.5 MW. In that same test cell there is another engine W20, which has a nominal rotation speed of 1000 rpm and a nominal power of 1.44 MW. It is connected to the external magnetized generator, which can supply power either to the grid or to load resistors with a nominal voltage of 10.5 kV.

3.2 Disturbance related components and equipment

This part describes in more detailed the components and equipment which might cause disturbances. This is done by focusing mainly on the components that are the source of either fast current or voltage oscillation or high currents or voltages. These components are the permanent magnet generator, the power converter and the power cabling between these two.

The disturbances have been present in the W20 engine's cylinder pressure measurement signals. Since the disturbances have appeared only when the WDF has been running, this indicates that the disturbances are likely resulting from electromagnetic emissions caused by the permanent magnet generator. The Converter is located in a separate converter room, which means that the emissions could originate either from the permanent magnet generator or the cabling between the generator and the converter. The cylinder pressure measurements are taken by 0-10 V analogy signal. Measurements are sensitive since they need to react fast for instantaneous pressure changes, which might be the reason why disturbances are present only in these signals.

Figure 11 shows a principal drawing of a generator connection to a switchgear. The link between the generator and the frequency converter is done by 20 pcs of MCCMK3x185+95 cables. Since the generator consists of double set of supply windings, it means that there are 10 pcs of three phase cables connected for each set. Three phases are in the same cable, which is meant to minimize the H-field caused by the cabling. The screens of the cables are connected to the earth only on the converter side, the generator side is floating. This kind of screen connection makes the screening to block only the E-field, not the H-field caused by fast current oscillation. These cables are installed to three cable ladders which are running near the roof top, all ladders mounted on top of each other, in the way shown in figure 12. The distance between the three cable ladders is about 30 cm. Even though this cabling is routed through another test cell no disturbances have been present in there.

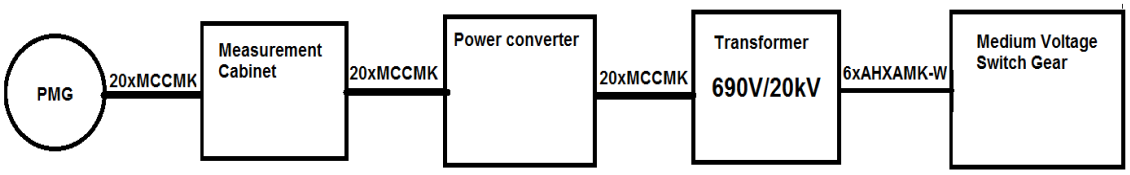

Figure 11. *The permanent magnet generator's single line drawing.*

The permanent magnet generator in use at the laboratory is a similar model that is presented in figure 12 below. The nominal frequency of the generator is 62.5 Hz, which it reaches by a 750 rpm rotating speed. The nominal output power of the generator is 5.5 MVA, the nominal current is 6 kA and the nominal voltage is 660 V. The generator consists of double windings. The EMC requirements for the generator are set by IEC 60034-1 rotating electrical machines part one - rating and performance. It determines the maximum emissions allowed for the brushless generator, which should comply with the requirements set by CISPR 11, Class B, group 1 [6]. These requirements are shown in table 3.

Figure 12. *A permanent magnet generator [16].*

Table 3. *The emission limits set by IEC 60034-1 [6].*

	Frequency range	Limits
Radiated emission	30 MHz to 230 MHz	30 dB(μV/m) quasi peak, measured at 10 m distance (Note 1)
	230 MHz to 1 000 MHz	37 dB(μV/m) quasi peak, measured at 10 m distance (Note 1)
Conducted emission on a.c. supply terminals	0,15 MHz to 0,50 MHz Limits decrease linearly with logarithm frequency	66 dB(μV) to 56 dB(μV) quasi peak 56 dB(μV) to 46 dB(μV) average
	0,50 MHz to 5 MHz	56 dB(μV) quasi peak 46 dB(μV) average
	5 MHz to 30 MHz	60 dB(μV) quasi peak 50 dB(μV) average
NOTE 1 May be measured at 3 m distance using the limits increased by 10 dB. NOTE 2 Emission limits are from CISPR 11, Class B, Group 1.		

The converter system used for converting the power generated by the permanent magnet generator is a liquid cooled converter. This power converter is designed for energy production applications such as wind power production. The converter's function is to adjust the load for the generator, i.e. the current the converter is supplying to the grid [3, p.3]. In this application, the converter is set to convert the generated power with varying frequency to constant 50 Hz frequency. The converter is located, in a separate room with a step-up transformer. The applicable EMC standard is IEC 61800-3, which is a specific standard for adjustable speed electrical power drive systems. Complying with this standard means that the converter should have current THD less than 5 % [3, p.14]. The converter contains filtering on both generator and line side connections. The line filtering is meant to attenuate both the common- and the differential mode emissions, the generator side filtering is meant to attenuate only the differential mode emissions. The frequencies these filters are meant to attenuate remains unknown. [21]. Figure 13 presents an example of a power converter manufactured by The Switch.

Figure 13. *A full power converter manufactured by The Switch [22].*

3.3 Cylinder pressure measurement system in test cell 3

This part introduces disturbance related components. The setup where disturbances have been present is a circuit which is used to measure W20 engine's cylinder pressure. The disturbances disappeared by re-routing cylinder pressure signal cables.

The disturbed measuring circuits were formed by: cylinder pressure sensors, Kistler 1704A4 Triaxial sensor cables, a rack amplifier and coaxial cables. The pressure sensors were connected through the triaxial cables to the rack amplifier. From the rack amplifier, the signal ran through the coaxial cable to a AVL-Indimodul measuring device, which located in the control room. These coaxial cables were installed to the signal cable ladders that are mounted only 20 cm below the lowest of the three power cable ladders. The co-axial cables were installed for a length of approximately 4 meters to run under the power cable ladders.

Afterwards the measuring circuits were entirely re-routed which made the disturbances disappeared. Figure 14 presents the power cable ladders. According to the classifications presented in chapter 2, power cables can be classified as class 4, and coaxial cables can be classified as class 2 cables. For these classifications the separation distance between the cables should be at least 50 cm.

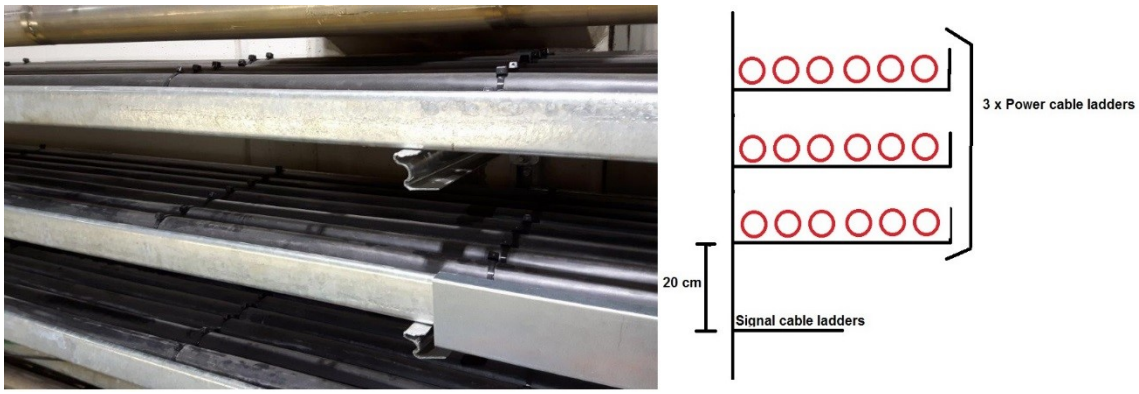

Figure 14. *The power cable ladders.*

The cylinder pressure measurements are recorded, transferred and modulated through the AVL Indimodul 621 multiple channel indicating system to data type which can be transferred through bus for further use. The AVL Indimodul records measurements based on crank shaft angle, which makes it possible to know timing for each sample [12, p. 17]. AVL Indimodul 621 includes low pass filter with 100 kHz cut-off frequency [12, p.39]. Before re-routing the cables from the rack amplifier they were running through test cell 3 to control room, where the AVL Indimodul was located. At the re-routing the AVL Indimodul was mounted to the side of the W20 motor, where the cylinder pressure signals run straight from the cylinders to the AVL Indimodul, not through cable tray. By this way, also the length of the cabling remains short and there is no parallel run with the power cables. From the AVL Indimodul the measurement signals are tracked through a bus to the control system.

3.4 Disturbances present in test cell 3

This part presents the records from the disturbances that have been present in cylinder pressure measurements. Since the measuring circuits were re-routed, one additional cylinder pressure sensor was installed to simulate the original situation.

The disturbances that occurred during the test periods are presented in figure 15 below. These disturbances have already been fixed by re-routing W20 engine's cylinder pressure signal cables. Therefore, this is the only disturbance record from the situation, where disturbances were present. Measurement was taken every 0.0000833 s at the rated speed of 1000 rpm, since the sampling interval of the measurement was 0.5 crank shaft angle degrees. According to the Nyquist sampling theorem the sampling frequency should be at least twice the highest frequency the signal contains for correctly representing the signal [10, p.1]. The sampling frequency can be calculated by equation 7 presented below, where f is sampling frequency and t is sampling interval. Substituting t= 0.0000835 s to equation 7 results f=12 kHz. Based on figure 15 the sampling frequency is not high enough for the disturbance voltages and thus aliasing occurs. This makes the disturbance record insufficient for determining the emission frequencies.

$$f = \frac{1}{t} \qquad (7)$$

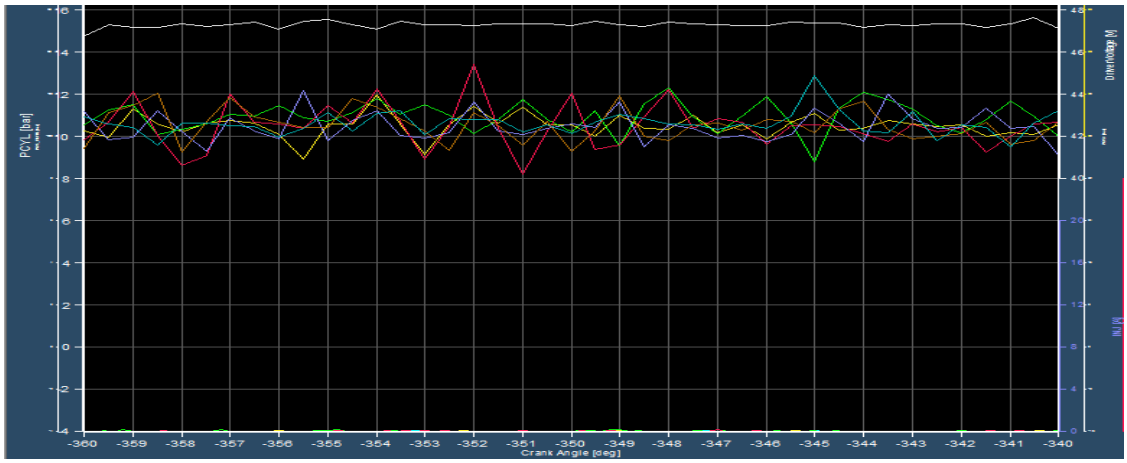

Figure 15. *A disturbance record with the sampling frequency of 12 kHz.*

For more accurate measurements one additional cylinder pressure sensor was installed to the W20 engine's cylinder and a cable from it was routed back to the former route to the control room, where it was connected to an AVL Indimodul measuring device. The AVL Indimodul was set to do sampling every 0.00125 ms, which according to equation 7 means 800 kHz sampling frequency. It was the fastest set up option and was meant to give as accurate measurements as possible. Test was done by running the WDF engine while the W20 engine was standing still. In other words, only coupled disturbances were present because there were no pressure changes in the cylinder of W20 engine.

Figure 16 presents the disturbance record taken with AVL Indimodul. According to equation 7 the frequency of the disturbances is higher than 50 kHz. In this record the sampling frequency should be fast enough to get reliable results of the frequencies emissions consist of. However, what needs to be taken into account, is that the AVL indimodul includes a low pass filter which attenuates frequencies above 100 kHz. This leads to situation where the record might not show all frequencies with severe disturbances.

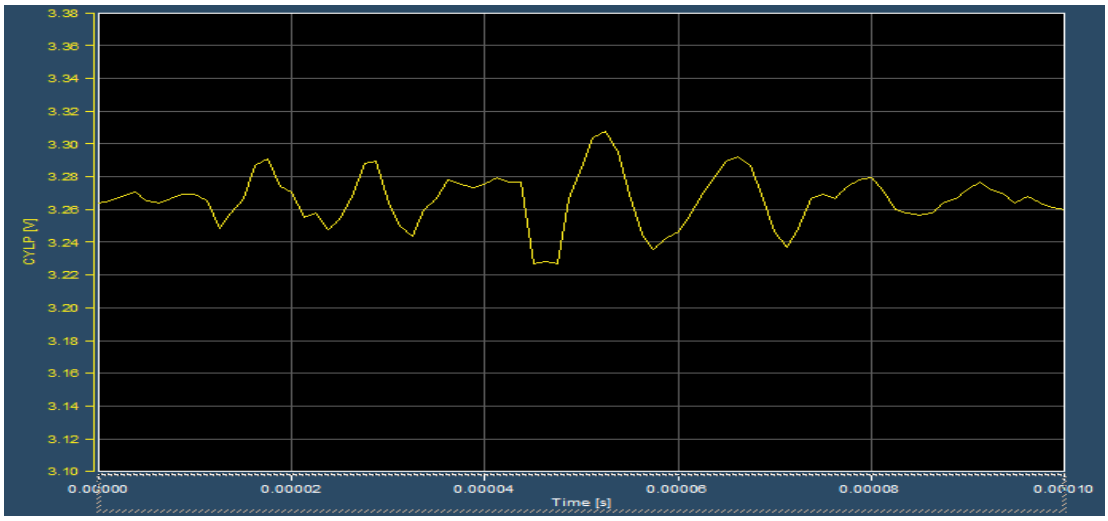

Figure 16. *A disturbance record with the sampling frequency of 800 kHz.*

4. MEASUREMENTS OF ELECTROMAGNETIC EMISSIONS

It is easier to solve the issues related to the electromagnetic emissions if the exact source and frequencies of severe disturbances are known. The origin can be detected by measuring the electromagnetic radiation from the test cell with the spectrum analyser or an oscilloscope. This chapter presents the measurements taken from the engine laboratory, shows the results and analyses the behaviour of the emissions presented in the laboratory.

4.1 Oscilloscope measurements in test cell 3

The AVL Indimodul did not offer measurements accurate enough for further analysis. Because of this, additional measurements were needed. An oscilloscope presents the entire disturbance signal without significant attenuation. This is the reason why the oscilloscope measurements presented in this chapter became necessary.

To get more information regarding the disturbances that occurred in measurements presented earlier, one cylinder pressure sensor was connected to coaxial cable which was installed to run along the signal cable ladders. These were the same signal cable ladders where the cylinder pressure cables were when the disturbances were present. This coaxial cable runs the length of 6 meters under the power cable ladders. Figure 17 presents the test set up. This set up differs little from the original situation, since instead of a rack amplifier, there is a single channel amplifier in use. This should not make any difference to coupling of disturbances. The cabling between the amplifier and the oscilloscope is done with the coaxial cable and the cabling between the amplifier and the sensor is done by Kistler triaxial cable. With this set up, it was possible to simulate the disturbances that have coupled to the sensor cables before the re-routing, and tests regarding how different screening actions affect the disturbances were much easier to perform. All measurements were taken when W20 engine was standing still.

Measurements were taken with Tektronix DPO 4034 digital phosphor oscilloscope. Measured mean RMS values are the only reliable measurements presented in the figures taken, since the wave form of the disturbances is unpredictable, which made peak to peak and amplitude values inaccurate. This is why this study uses only RMS mean values measured with an oscilloscope for analysing the measurements.

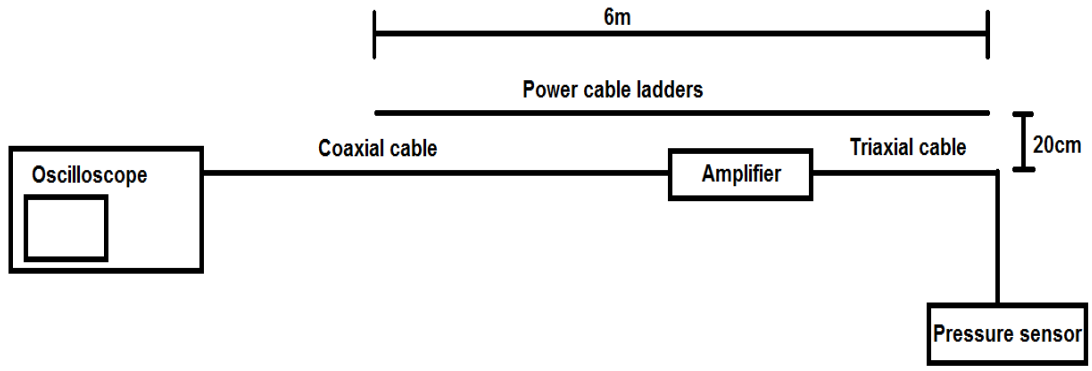

Figure 17. *The test setup of the oscilloscope measurements.*

Measurements were taken while the WDF engine running with full load without additional screening. Figure 18 presents the waveform acquired from this situation, cursors are set to measure the wave period of the most severe disturbance frequency. The cursor measurement shows that one period takes 12.24 µs, which indicates a frequency of 81.7 kHz.

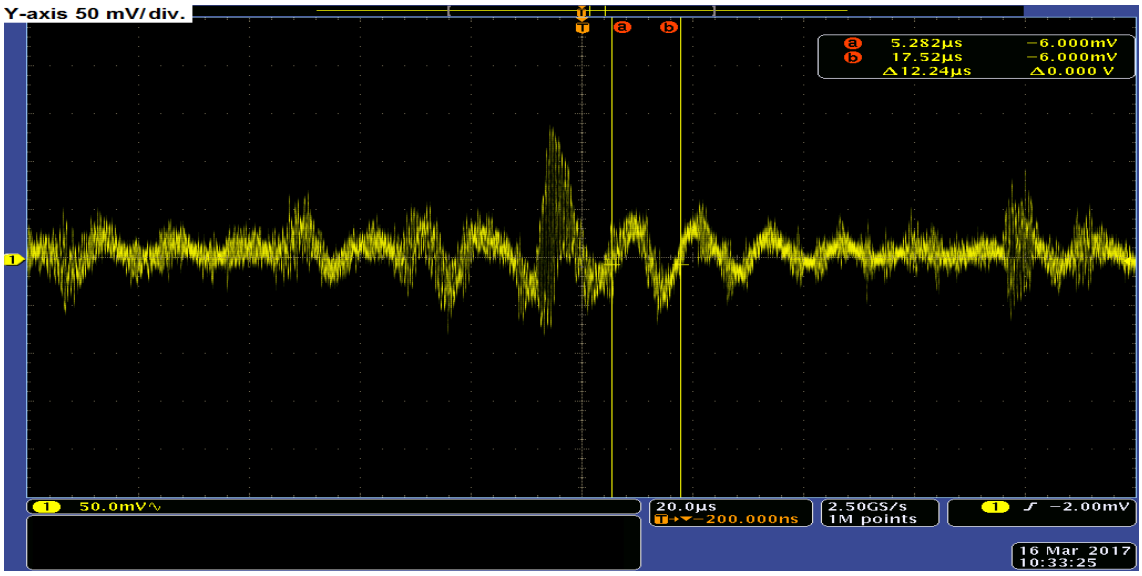

Figure 18. *The wave period measured with cursors, 100 % load, 20 µs/div.*

For presenting the effects of load change the oscilloscope measurements were taken while the WDF engine was running with 0 % (1 kW) and 100 % (5.5 MW) loads. Figures 19 and 20 are presenting how the reduced load affects to induced disturbances. These measurements are presented also in table 11 in appendix A. Table 11 shows that the induced disturbance voltage is reduced by 26 % when the load is adjusted from 100 % to 0 %. According to these measurements, load changes are not affecting with the same ratio to induced disturbance voltage. It is difficult to make any further analysis based on these measurements.

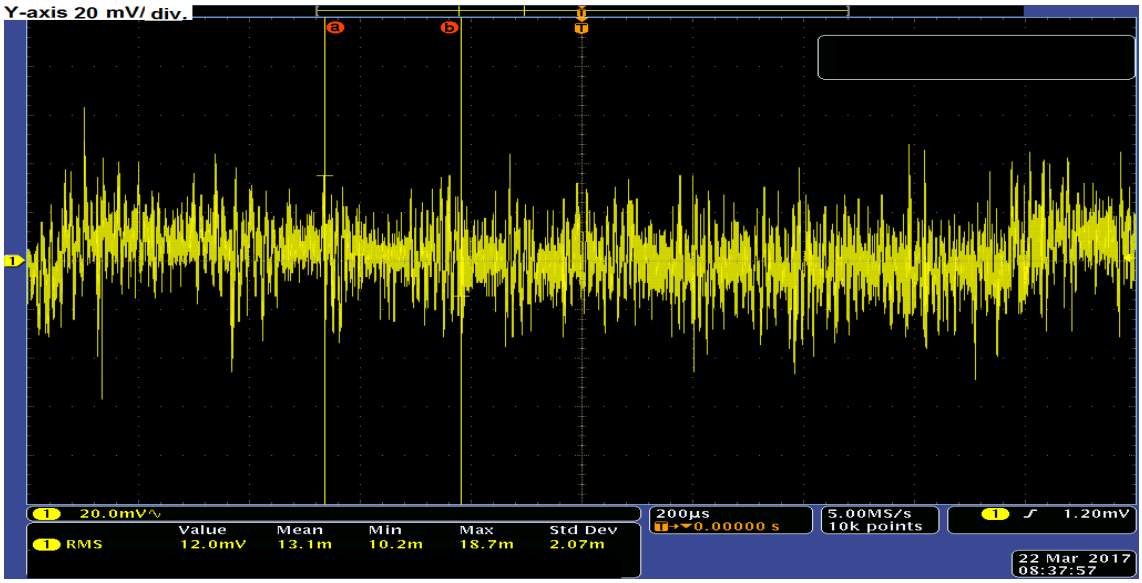

Figure 19. *The engine run. with 0% load, no additional screening provided, 200µs/div.*

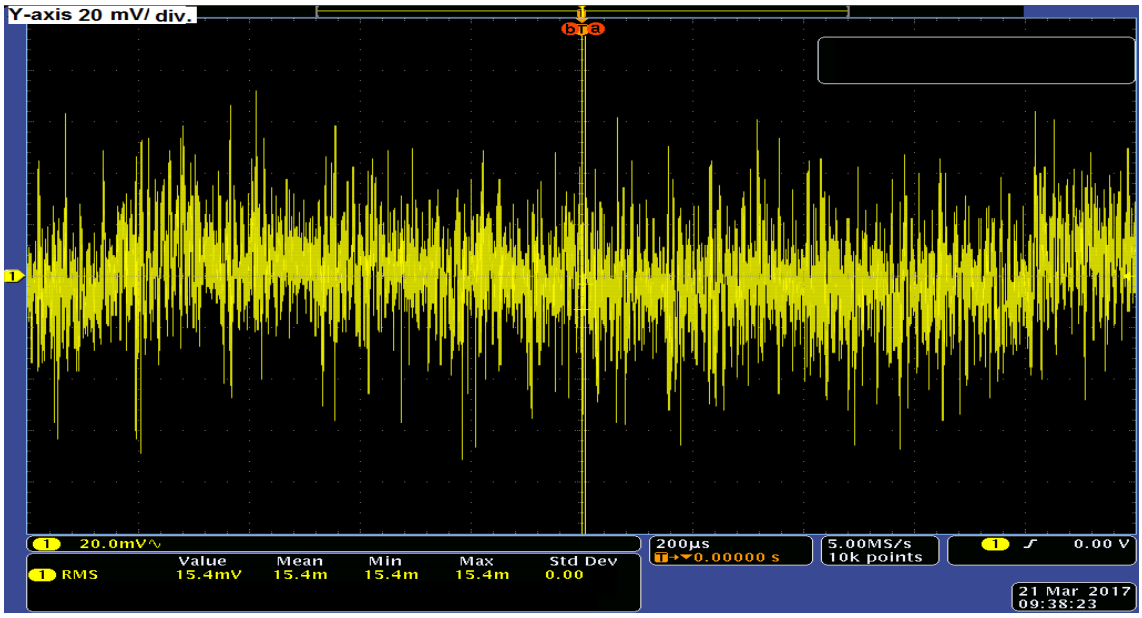

Figure 20. *The engine run. with 100% load, no addit. screening provided, 200µs/div.*

The oscilloscope measurements were taken also in conditions where the generator of the WDF was standing still, for defining the disturbances that does not originate from the permanent generator or the cabling. Figure 21 presents the measurements taken from this situation. According to figure 21 the pressure sensor itself creates a disturbance voltage of 6.67 mV. The source of this might be the external amplifier. Comparisons regarding the oscilloscope measurements are presented in table 11 in appendix A. In table 11 normalized disturbance voltage value is based on the situation where generator was standing still. This is calculated by subtracting the measured RMS voltage when permanent magnet

generator was standing still (6.69 mV), from the measured RMS voltage from each situation. Table 11 presents that the normalized disturbance voltage while the engine was running on full load was 8.73 mV, which is 57 % from total RMS voltage measured.

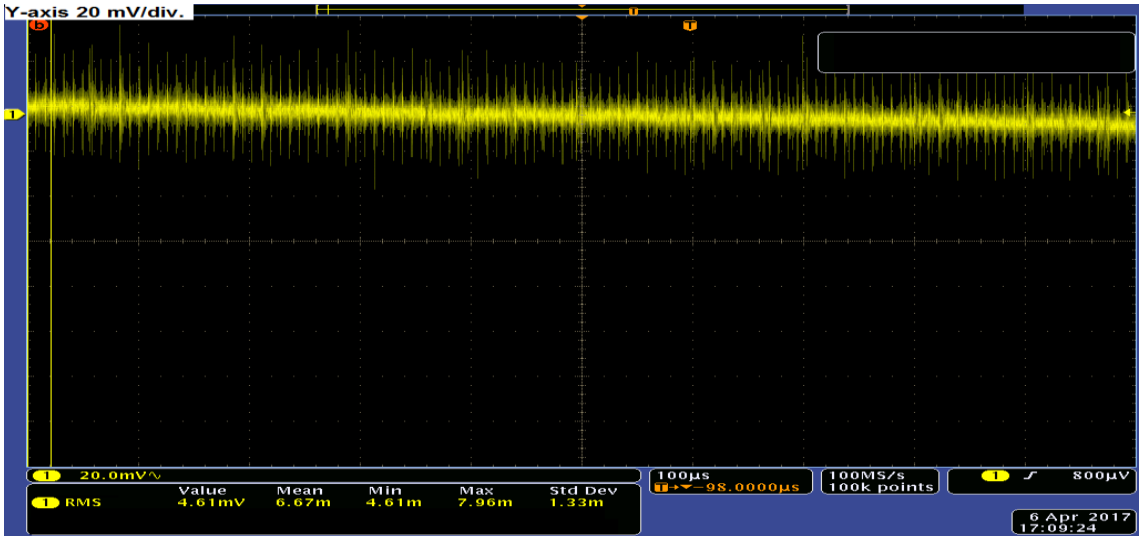

Figure 21. *The permanent magnet generator standing still, 100 µs/div.*

4.2 Spectrum analyser measurements in test cell 3

For further analysis, high frequency electromagnetic emissions were measured with a spectrum analyser, it is a relevant device for determining behaviour of emissions caused by H- and E-fields, frequencies of the emissions and for localizing the source of the emissions.

The spectrum analyser used for these tests is Tektronix model RSA306 B. The measurement range of this analyser is from 9.5 kHz up to 6.2 GHz, so it should be capable of tracing of the origin the high frequency emissions and defining the most harmful emission frequencies. For measuring with the spectrum analyser, the near field probe set Electro Metrics EHFP-30 is used to connect the emissions to the spectrum analyser, from the probe set 1 cm ball probe is used for measuring the E-field emissions and the 6 cm loop probe is used for measuring the H-field emissions. The probes were chosen because these were the largest ones, and since the larger probes should provide increased sensitivity [7]. Measuring probes are connected via a coaxial cable to the spectrum analyser. Attenuation of coaxial cable was measured with a function generator. This was done by supplying certain voltage and comparing this to the values spectrum analyser measured. In this case the frequency of 100 kHz was supplied, which resulted a -2.2 dB cable attenuation. This means that due to the coaxial cable and its connections 2.2 dB have to be added to measured values. This and the antenna factor of the H-field probe were programmed to the spectrum analyser`s settings, which adds them automatically to the measured values. Since antenna factor was not available for to E-field probe used, only the coaxial cable

attenuation was set when E-fields measured. Because of this, the E-field measurements are inaccurate, and the results are reliable only for determination of the emissions source and for analysing the effectiveness of screening actions. Figure 22 presents the near field probes that are used on spectrum analyser measurements.

Figure 22. *The near field probes used for the spectrum analyser measurements.*

The concern regarding the spectrum analyser measurements was that all measurements should be taken from exactly the same measuring points to get comparable results. During these measurements the W20 engine was standing still. To get knowledge on whether the permanent generator is the source of the emissions, measurements were taken once with a 0 % load and while the generator was standing still. In all measurements taken with the spectrum analyser the measured peak values are presented as a blue curve, and average RMS value from 10 samples is presented as a yellow curve. Markers are set to present the peak values from the measurements. There might be even higher values at the lower frequencies, but the spectrum analyser is not capable of reliably measuring at frequencies below 9.5 kHz. Measuring devices for measuring emissions with lower frequencies were not available. Most measurements were taken with the range of 9.5 kHz to 200 kHz, since most severe emissions were in this range.

The selected measuring points around the WDF engine are presented in figure 23, these places were around the engine selected because it was easy to do measurements from there and to achieve most relevant measurement data. Measuring points A & B were chosen just to show that most of the high frequency emissions originate from the power cabling, not from the generator. This is the reason why A & B are not taken into account when effects of screening or load changes are analysed. Loop probe measurements depend on the orientation of the loop. The measurements are taken with the orientation that gives the highest measurement values, and then this orientation is applied each time measurement is done from the same point. Figure 24 presents the more specific points and the

way points C, D and E are measured. The current loop is attached in a way that its lower edge is aligned with the signal cable ladders frame bar's upper edge.

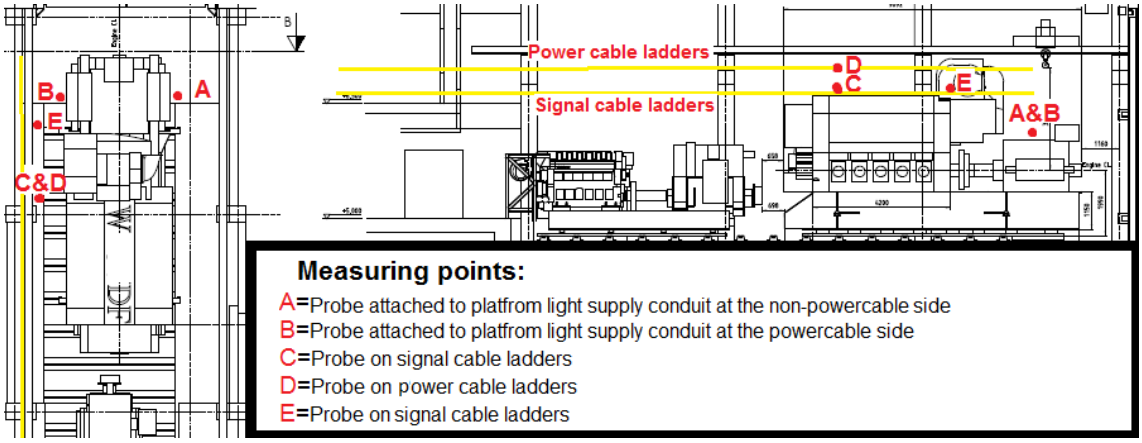

Figure 23. *The measuring points of test cell 3.*

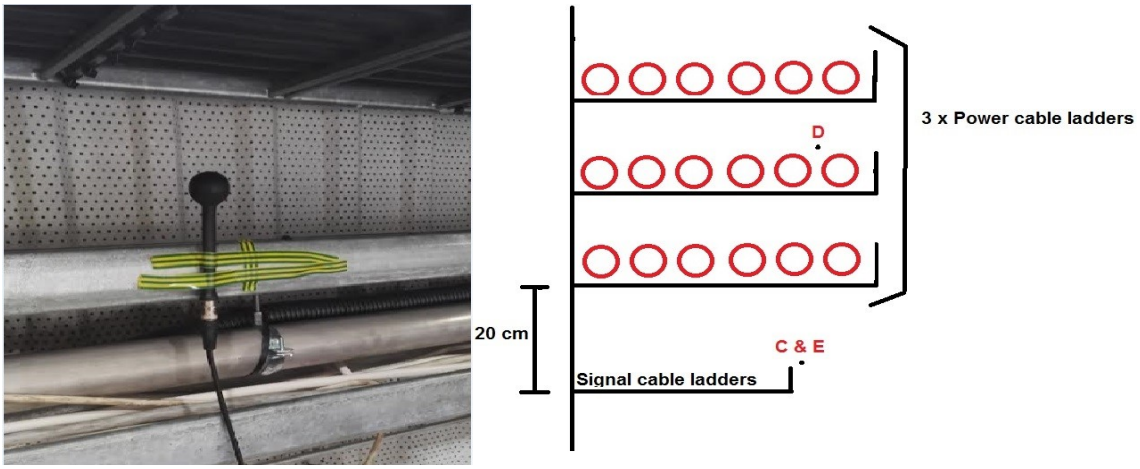

Figure 24. *A more detailed picture of measuring points C, D and E.*

The H-field measurements taken with the spectrum analyser are presented in dBµA/m units. These can be converted to more common µA/m units using equation 8, where H is the strength of the H-field, and Hdb is the measured H-field in dBµA/m units.

$$H = 10^{HdB/20} \quad (8)$$

Figures 25-30 present measurements taken when the WDF engine was running on 100 % load. All measured peak values are presented in table 9 in appendix A. Equation 8 transforms the highest peak value measured 92.3 dBµA/m to 41.21 mT/m. This was measured from the signal cable ladders from point E. It is a surprise that H-field measured from measuring point E was higher than any of values got near the power cables. From the point E, H-field was reduced from the peak value of 92.3 dBµA/m to 71.4 dBµA/m, when measurement was taken 10 cm below the signal cable ladders. The reason for this might be that point E is at the point where the steel structures are not blocking H-field caused by the power cabling, which leads to that the H-field somehow sums to this point. Another

possible reason for this could be insufficient earthing at the power cable ladders, which allows earth currents to flow through the cable ladder structures and cause H-fields. Overall measurements gave much higher values if they were taken near the power cables, which indicates that the source of the most severe high frequency H-field emissions is the power cabling.

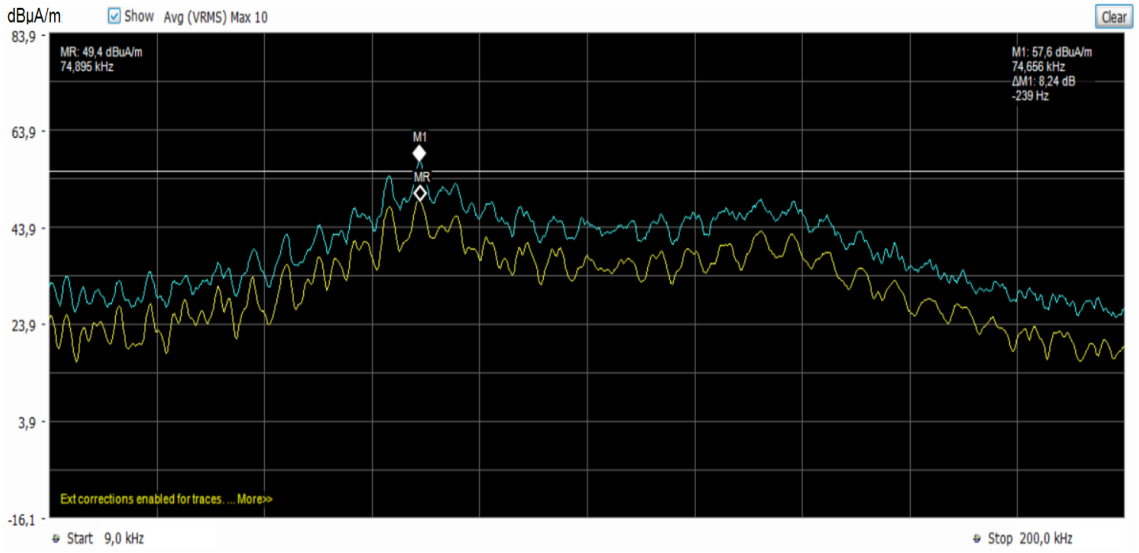

Figure 25. *H-Field measured from measuring point A, 9.5kHz-200kHz 100 % load.*

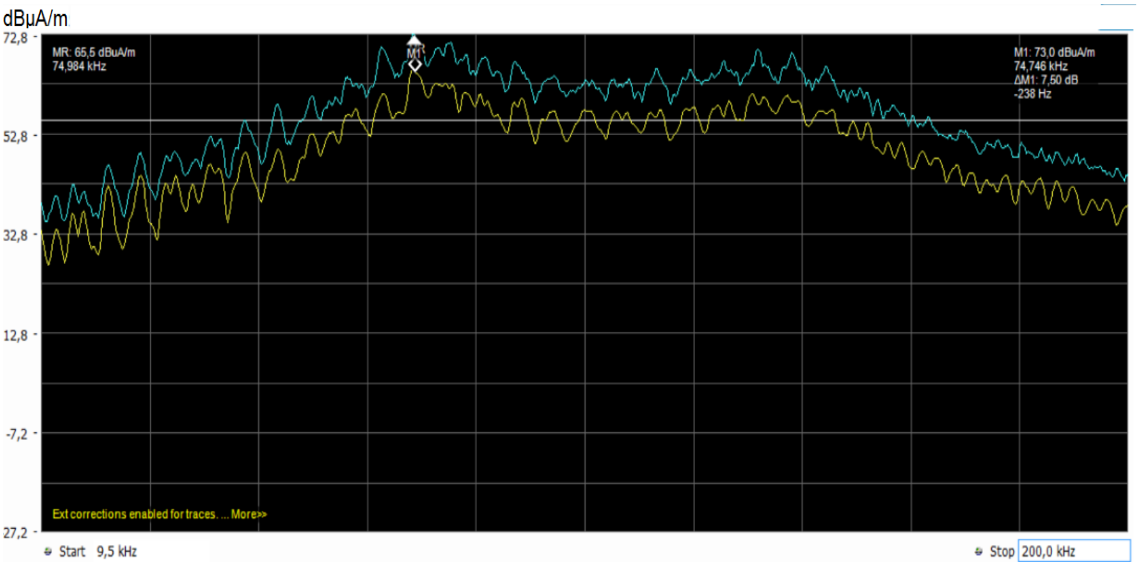

Figure 26. *H-Field measured from measuring point B, 9.5kHz-200kHz 100 % load.*

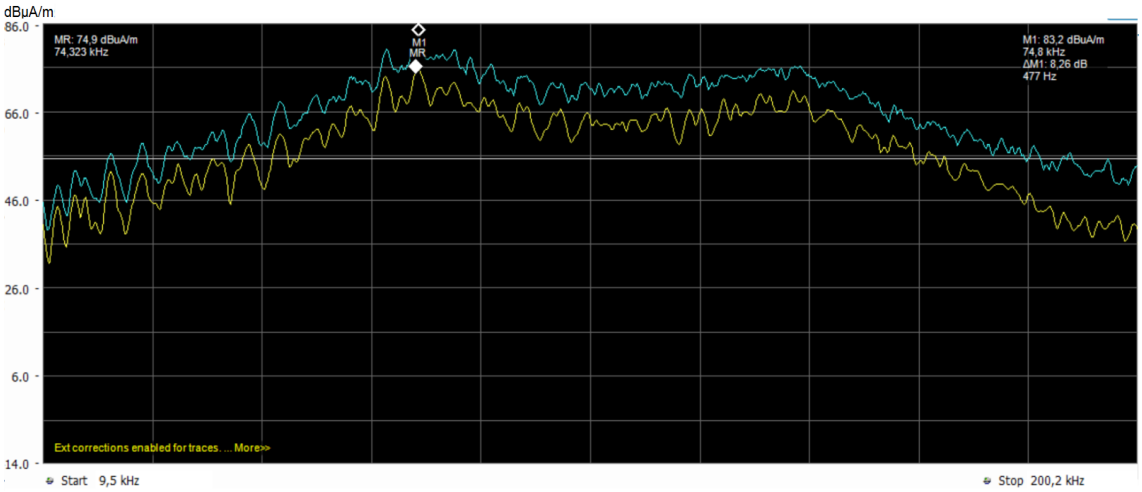

Figure 27. *H-Field measured from measuring point C, 9.5kHz-200kHz 100 % load.*

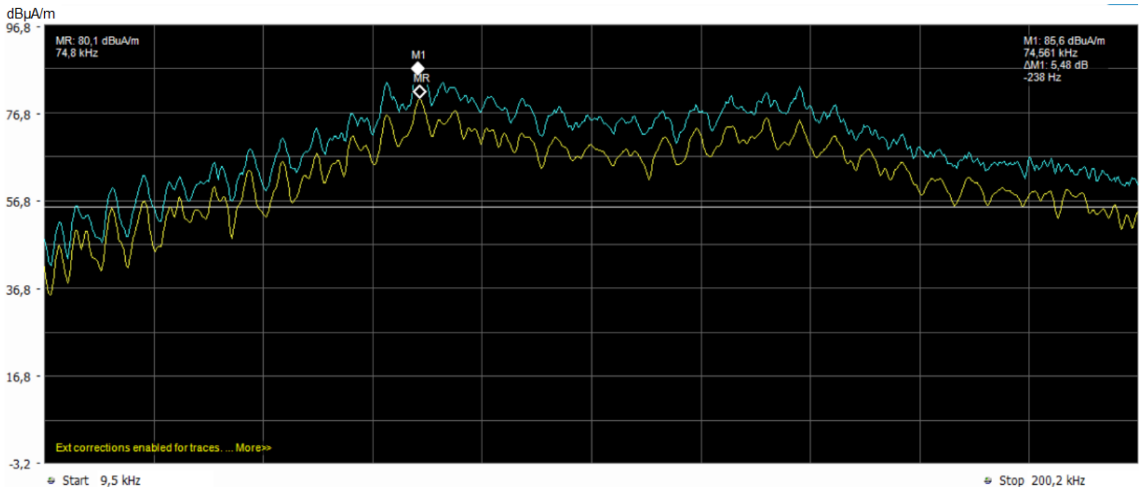

Figure 28. *H-Field measured from measuring point D, 9.5kHz-200kHz 100 % load.*

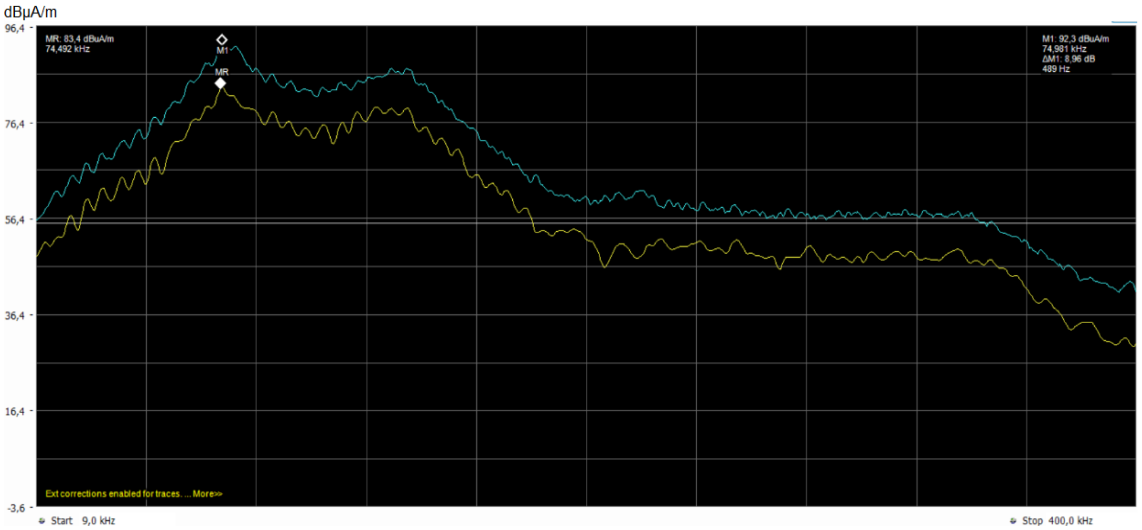

Figure 29. *H-Field measured from measuring point E, 9.5kHz-400kHz 100 % load.*

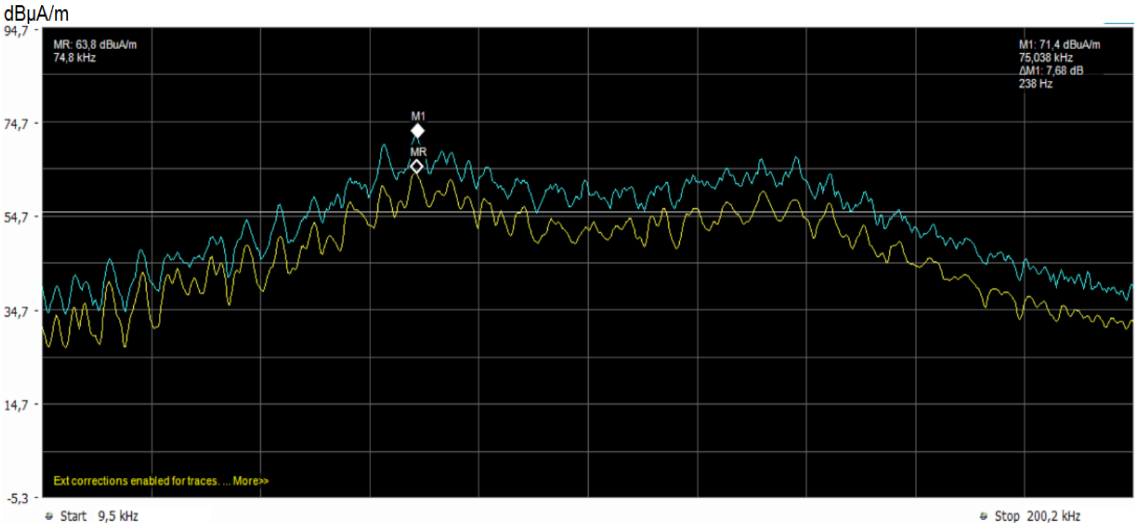

Figure 30. *H-Field measured 10 cm below the point E, 9.5kHz-200kHz 100 % load.*

E-Field measurements were taken from the same measuring points that H-field measurements were taken. The WDF engine was running with 100 % load during the measurements. These measurements are presented in figures 31-35 and measuring results are presented in table 9 in appendix A.

Measurements taken form the measuring point D, near the power cabling gave the highest E-field values, since it gave 2.788 mV peak value at the frequency of 141 kHz. In general, measurements taken near the power cabling gave higher values compared to measurements taken from the other side of the generator, similarly like it did with the H-field measurements. This is indicating that the source of the both H- and E-field emissions is the power cabling between the generator and the converter.

The frequency of the most severe emissions seemed to be quite similar at both H-field and E-fields near the power cabling. This frequency region is between the frequency of 65 kHz and 145 kHz. At this region H- and E- fields are forming two peaks, first at the frequency of approximately 75 kHz and the second at the frequency of 140 kHz. 75 kHz frequency is at the same range with the disturbance voltages induced to coaxial cable in oscilloscope measurements.

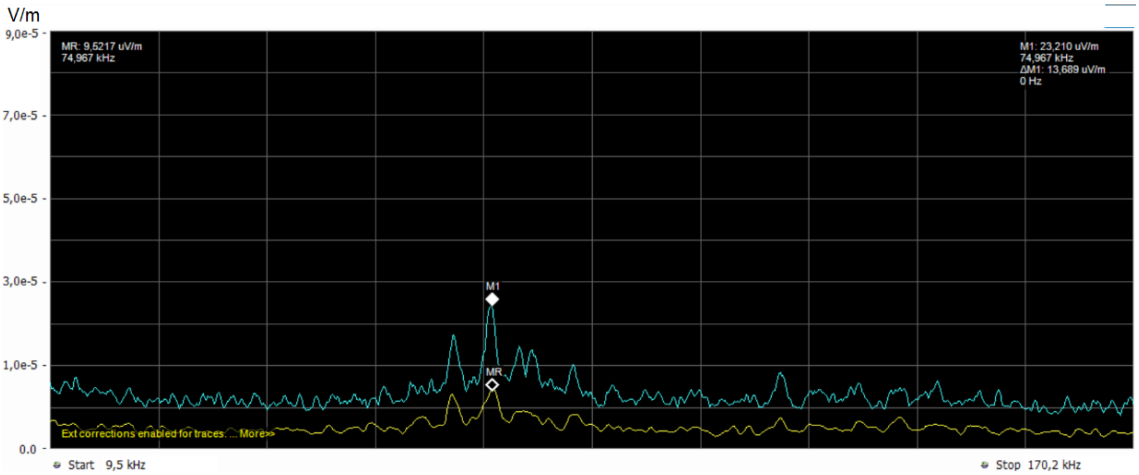

Figure 31. *E-Field measured from measuring point A, 9.5 kHz-170kHz 100 % load.*

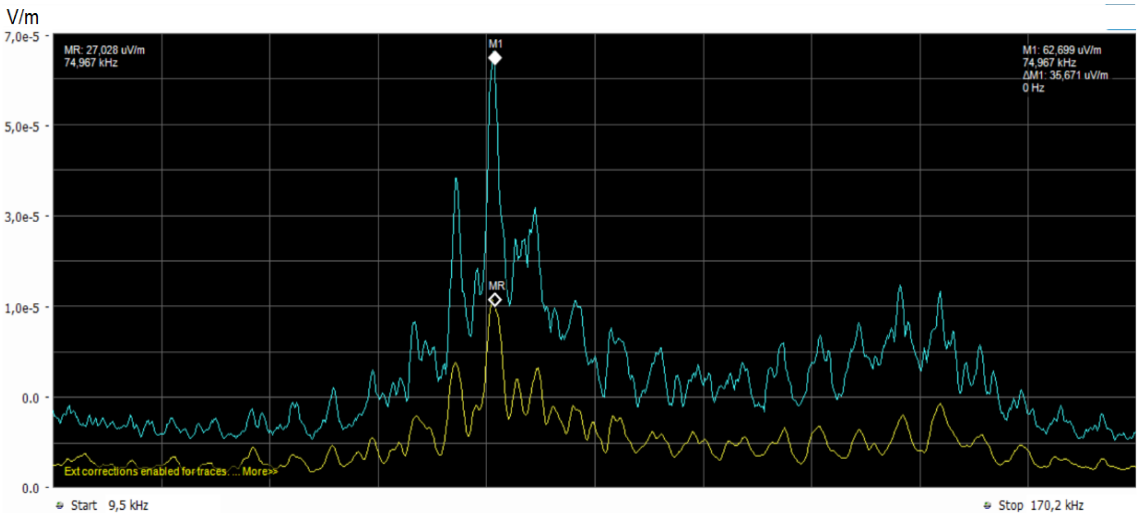

Figure 32. *E-Field measured from measuring point B, 9.5kHz-170kHz 100 % load.*

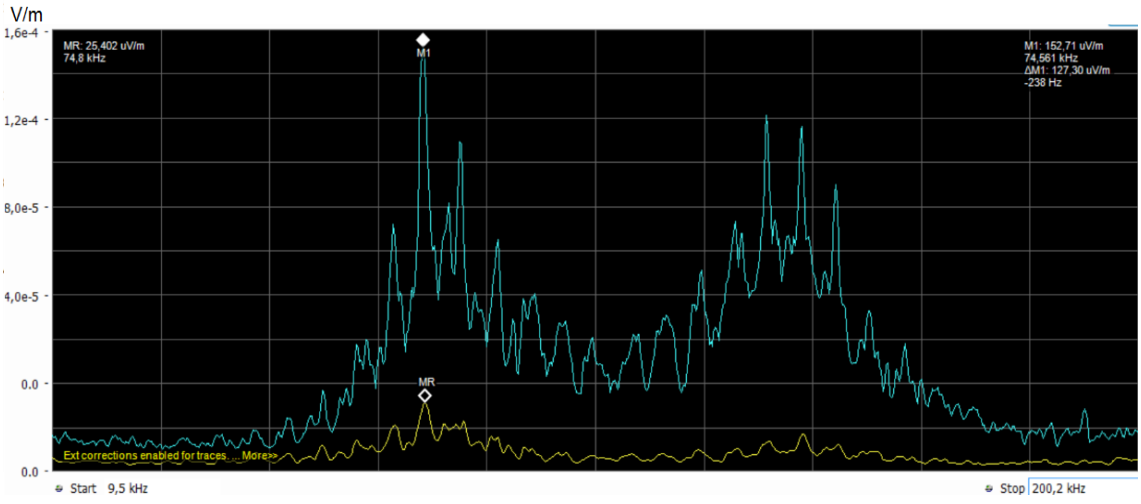

Figure 33. *E-Field measured from measuring point C, 9.5kHz-200kHz 100 % load.*

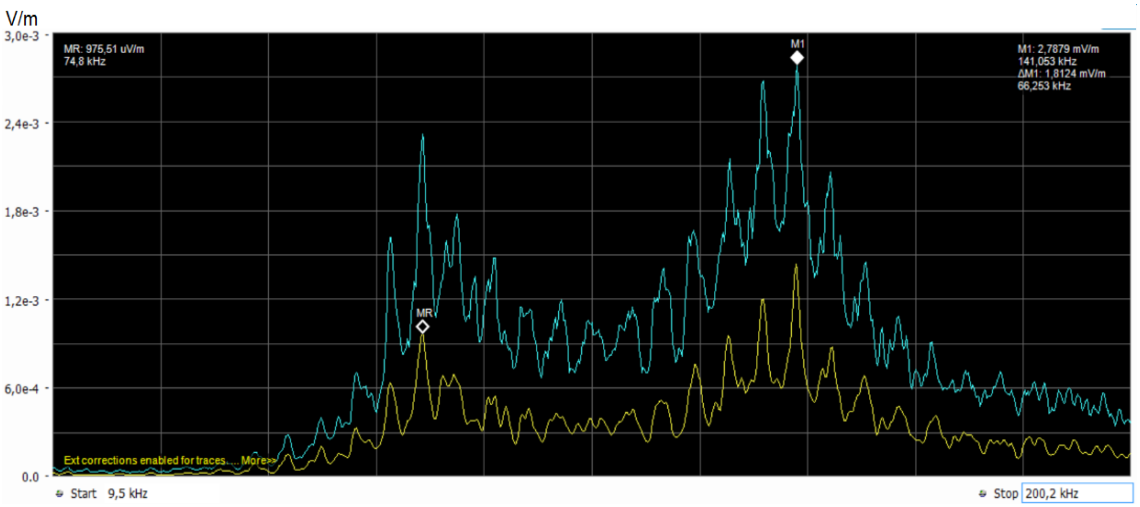

Figure 34. *E-Field measured from measuring point D, 9.5kHz-200kHz 100 % load.*

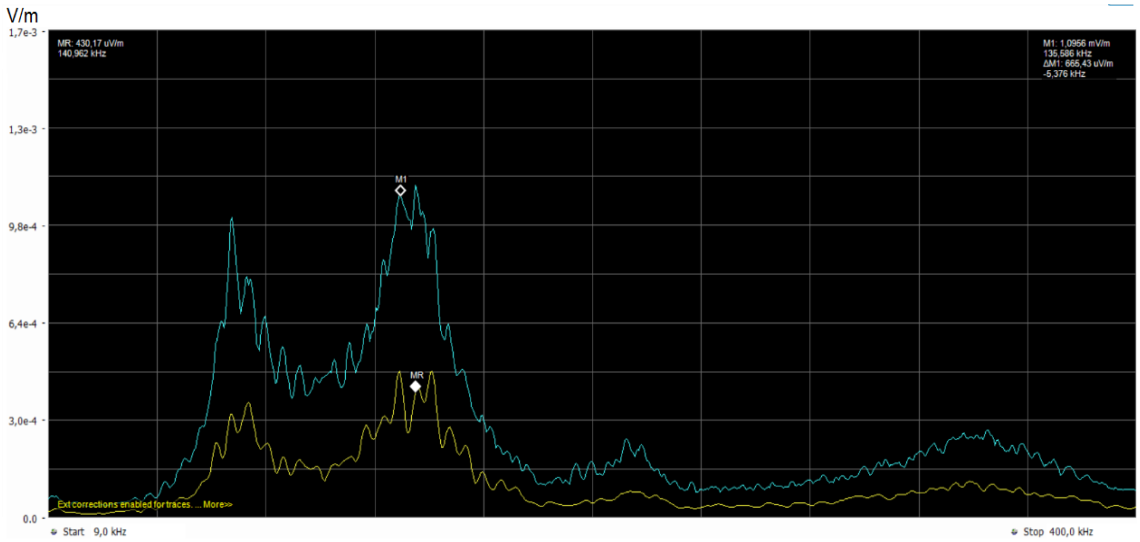

Figure 35. *E-Field measured from measuring point E, 9.5kHz-400kHz 100 % load.*

To clarify how load changes affect the high frequency electromagnetic radiation caused by the cabling and the generator, measurements were taken with 0 % (1kW) load. Results are presented in table 8 in appendix A. Measuring points A & B are not valid for this comparison, because external disturbances can have big influences to these measurements since measured values from these points were at such low level.

The effects of load change are presented in table 4 below. Equation 9 presents how the difference to full load values is calculated. In the equation 9, V_0 is the measured H- or E-field peak value when engine is running with 0 % load and V_{100} is peak value measured while engine was running with 100 % load. Equation 10 presents how change % values are calculated, where $Difference$ is difference value calculated in equation 9. All these values are presented in table 8 in appendix A. According to table 4, the high frequency H-field is decreased in points C, D and E when the load was reduced. Since the H-Field

is proportional to the current the result these measurements gave was not a surprise. It is surprising that changes were so modest. All values changed less than 45 %. The high frequency E-field reduced at points C and E, but point D stays nearly constant. The reason for the strange behaviour of E-field could be that in generally repeatability of E-field measurements is not good, which can make measurements inaccurate. According to these results, it seems that the emissions will remain present regardless of the load.

$$Difference = V_0 - V_{100} \quad (9)$$

$$Change\ \% = \left(\frac{Difference}{V_{100}}\right) \times 100\ \% \quad (10)$$

Table 4. *Effect of load change to high frequency emissions.*

Difference to full load values				
Point	µA/m	Change %	µV/m	Change %
C	-4896	-32%	-563	-42%
D	-5719	-30%	202	7%
E	-17767	-43%	-274	-25%

To verify that the permanent magnet generator and the power cabling are the sources of the high frequency emissions, all measurements were taken when generator was standing still. Measured values are shown in table 7 in appendix A. Like in the previous comparison, also in this the measurements taken from points A & B were not valid. The frequency spectrum was flat compared to the measurements taken when the engine was running, because of this peak values were measured in various frequencies, not at the specific frequency regions.

Table 5 below presents a comparison between the values measured when the WDF engine ran with 100 % load and the values measured when the generator was standing still. Equation 11 presents how the difference to full load values is calculated. In the equation V_{still} is the measured H- or E-field peak value when engine was standing still and V_{100} is the peak value measured when the engine was running on 100 % load. Equation 12 presents how change % values are calculated, where $Difference$ is difference value calculated in equation 11. Comparing measuring points C, D and E it seems that all high frequency E-field levels have reduced by at least 97 %, all H-field levels are reduced over 99 %. According to these measurements most of high frequency electromagnetic emissions present in test cell 3 are caused by the permanent magnet generator and the power cabling connected to it.

$$Difference = V_{still} - V_{100} \quad (11)$$

$$Change\ \% = \left(\frac{Difference}{V_{100}}\right) \times 100\ \% \quad (12)$$

Table 5. *Effects of the generator standing still for high frequency emissions.*

Difference to full load values				
Point	µA/m	Change%	µV/m	Change%
C	-15466.5	-99.86%	-1318.0	-98%
D	-19032.7	-99.89%	-2754.2	-99%
E	-41188.9	-99.95%	-1057.6	-97%

4.3 Measurements in the converter room

In the converter room, there are low voltage switchgears, one step-up and one step-down transformer and the power converter. Measurements taken from the converter room were taken with spectrum analyser and the magnetic flux density meter for analysing the effects of transformer and converter to propagation of emissions. All measurements were taken while the engine was running with full load. Measurements were taken all around the converter room. A couple of reference points were chosen from converter room. All the recorded measurements were taken from these points. Figure 36 presents the measuring points. Transformer is not in the picture since it locates on the platform which makes the second floor.

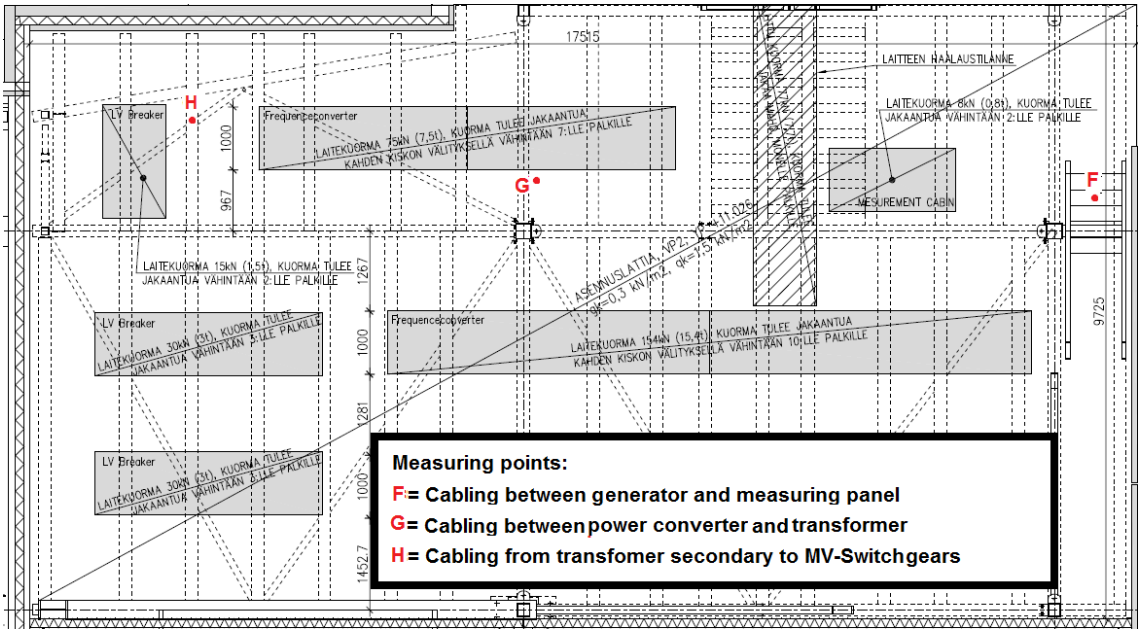

Figure 36. *The Measuring points of the converter room.*

High frequency H-field measurements were taken, results are presented in figures 37, 38 and 39, peak values as a blue curve and RMS as a yellow curve. The measurements were taken with 6 cm current probe, the WDF engine running with 100 % load. The results are presented in table 3 in appendix A. These measurements indicate that the transformer attenuates the high frequency H-field originating from the cables, since the H-field is

reduced from the 8318 µA/m (point G) measured before the transformer to a value of 15 µA/m (point H) measured from transformers secondary. The cables from the generator to the converter caused more high frequency H-field radiation than cables from the converter to the transformer. This could be because the grid side connection has both common and differential mode low pass filtering, the generator side connection has only differential mode filtering.

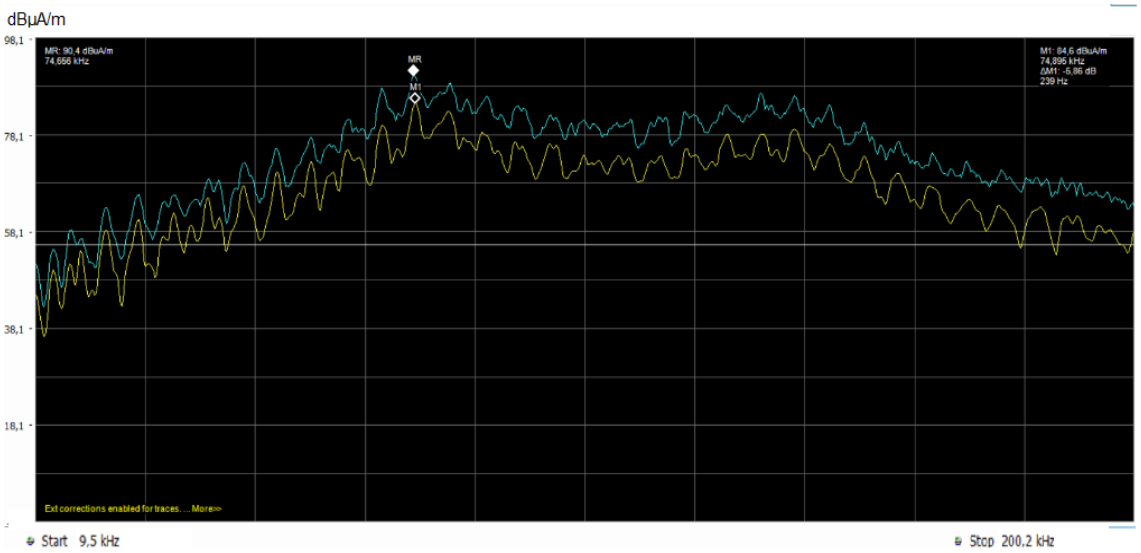

Figure 37. *H-field measured from measuring point F, 9.5 kHz-200kHz 100% load.*

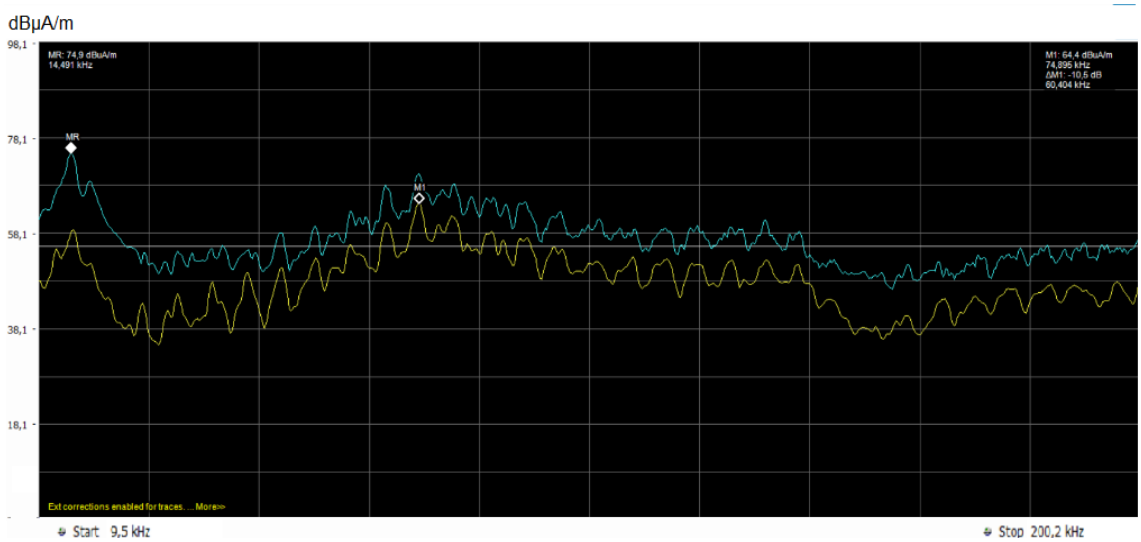

Figure 38. *H-field measured from measuring point G, 9.5kHz-200kHz 100% load.*

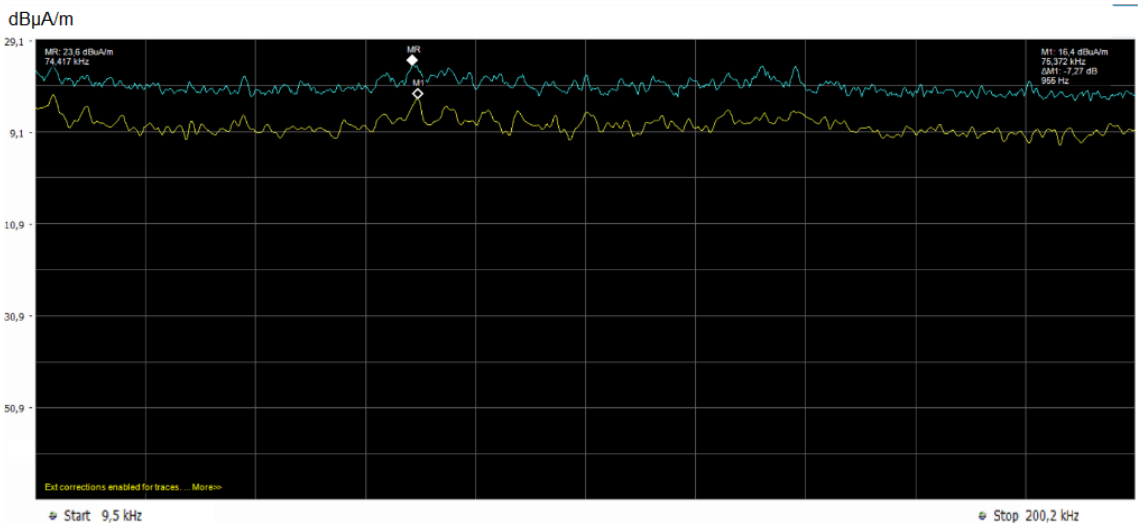

Figure 39. *H-Field measured from measuring point H, 9.5kHz-200kHz 100% load.*

High frequency E-Field measurements were taken from the converter room. Figures 40, 41 and 42 present the measurements. Measurements were taken with a 1 cm ball probe, results are presented in table 9 in appendix A. According to the measurements the power cabling between the converter and the generator is causing most high frequency E-field radiation, since the highest value 3.74 mV/m was taken from the measuring point F, measured near the cabling between the generator and the converter. The reason for this could be same as with H-field measurements. The supply filtering at generator connection might be insufficient. Overall the power cabling connected to the converter gave higher values than other components in the converter room.

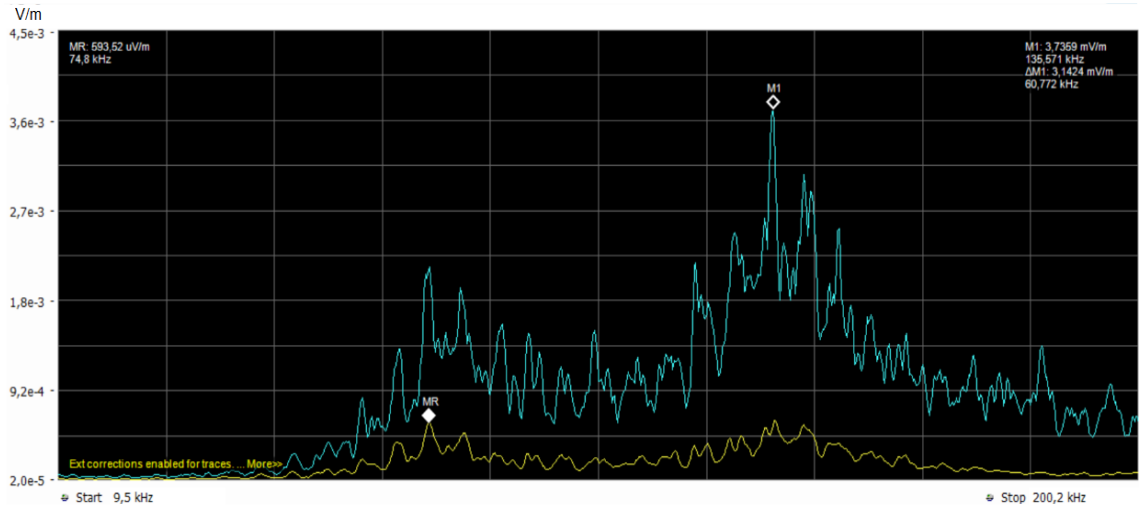

Figure 40. *E-field measured from measuring point F, 9.5kHz-200kHz 100% load.*

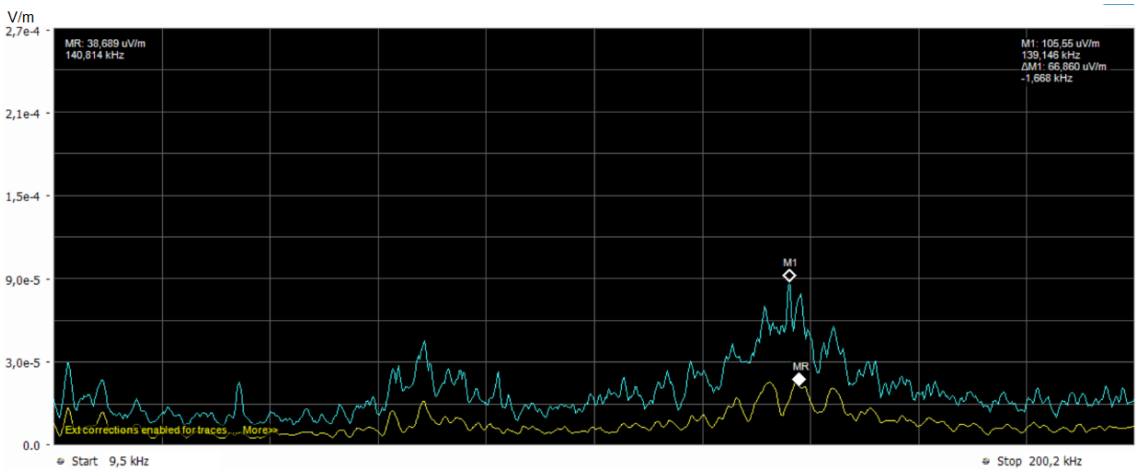

Figure 41. *E-field measured from measuring point G, 9.5kHz-200kHz 100% load.*

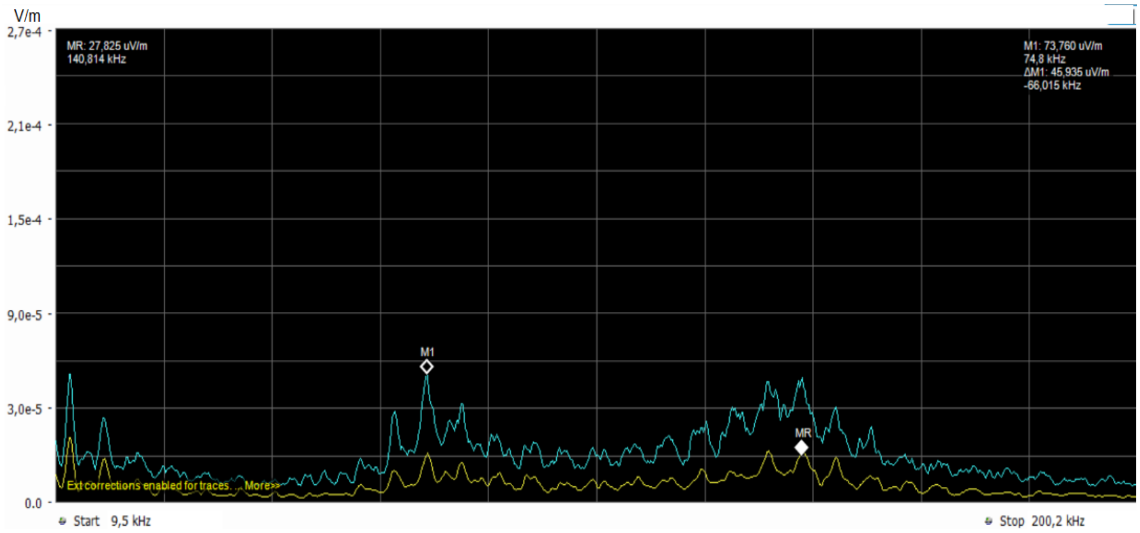

Figure 42. *E-field measured from measuring point H, 9.5kHz-200kHz 100% load.*

4.4 Measurements on the external magnetized generator

This part focuses on measurements taken form the external magnetized generator. This is because one aim of this study was to make a comparison between electromagnetic emissions originating from the permanent magnet generator and the external magnetized generator.

The engine generator set which was tested consisted of WSG engine and a 10 MVA generator manufactured by ABB. This setup was tested with a spectrum analyser and a magnetic flux density meter. Measurements taken with the magnetic flux density meter are analysed in the next subchapter. Since there were no external magnetized generators used in the engine laboratory at the time tests were done, these measurements were taken from

the test area of manufactured engines. All measurements were taken while the engine was running with a 7.85 MW load.

The setup was tested with spectrum analyser by trying to find points which gave noticeable high frequency emissions. The point where most high frequency emissions were measured was the point where power cables were coming from the supply terminals. Figures 43 and 44 present the measured E- and H-field emissions from this point. As these figures show, the spectrum is flat since there are no specific frequencies causing either severe E- or H-field high frequency emissions to the environment. This is a clear difference compared to emissions caused by the permanent magnet generator and power converter, since there was a certain frequency region which caused most electromagnetic radiation. Measured values 27.22 µA/m and 21.44 µV/m are at a similar level to values taken when the permanent magnet generator was standing still at test cell 3. This suggests that the synchronized external magnetized generator is not causing noticeable high frequency emissions like permanent magnet generator did.

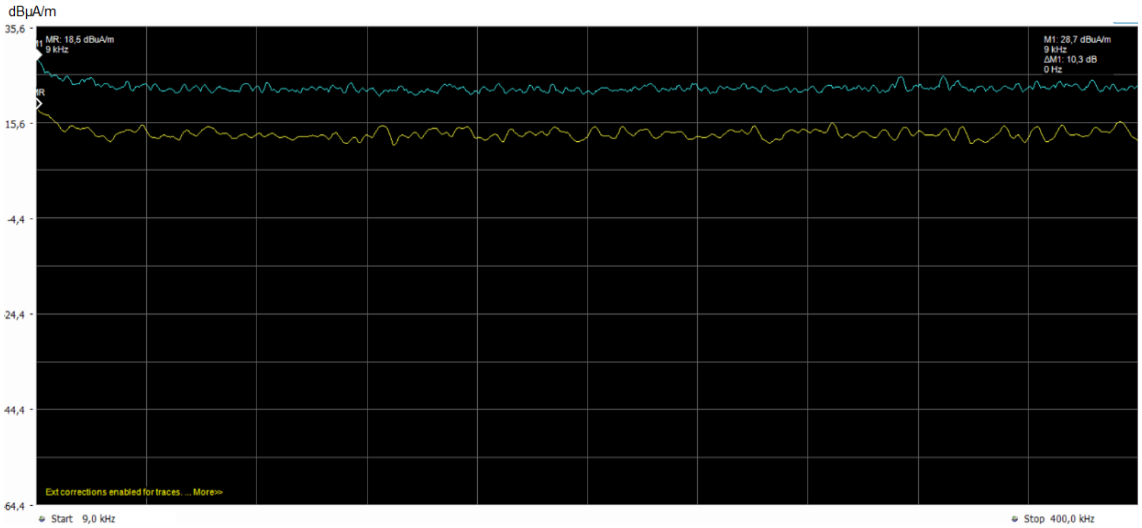

Figure 43. *H-field, near the generator's supply cabling 9.5kHz-400kHz, 100% load.*

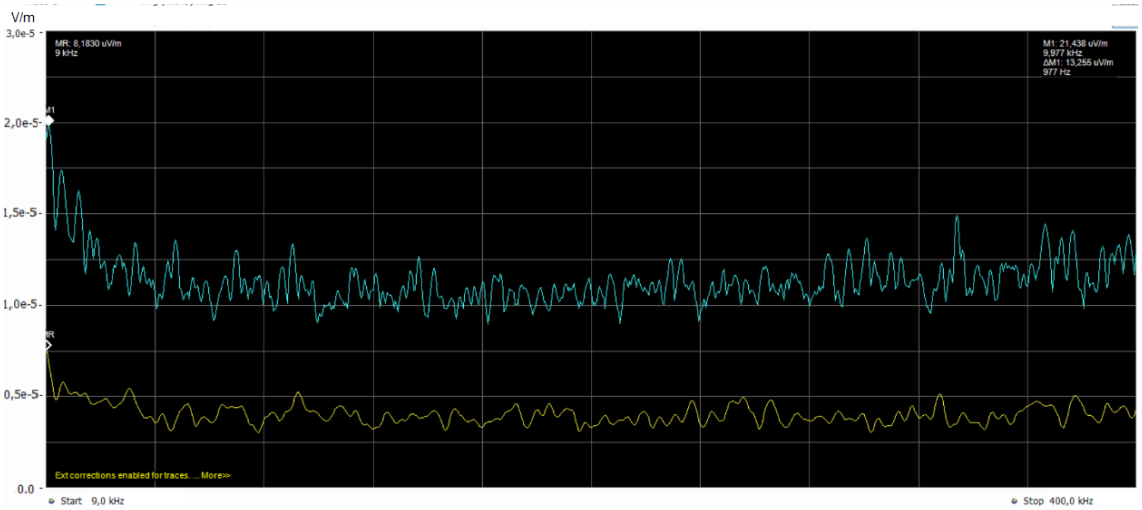

Figure 44. *E-field, near the generator's supply cabling 9.5kHz-400kHz, 100% load.*

4.5 Measurements related to health and safety

This part focuses on verifying whether the laboratory fulfils the requirements set by the Ministry of Social Affairs and Health in Finland regarding electromagnetism. This is done by focusing mainly on the H-field limits since measuring devices for measuring low frequency E-field, static H-field and magnetic flux density out of Hioki's range were not available. High frequency E-field measurements were not applicable for this purpose since the manufacturer did not provide the antenna factor for E-field probes.

Magnetic exposure measurements were done with a Hioki 3470 magnetic flux density meter. All measurements were taken while the engine was running with full load to get most H-field emissions. Measuring was done by trying to find the highest values for magnetic flux density and by observing magnetic flux changes at varying measuring points. All measurements with the Hioki 3470 were taken with a frequency range of 10 Hz-2 kHz. When measured with the frequency range of 10 Hz -2 kHz the analysis assumes that at least 95 % of the measured magnetic flux density in the circuit where the converter is involved in is composed of a fundamental wave. This is based on the fact that by complying the IEC 61800-3, power converter should allow for maximum 5 % of current THD. For the external magnetized generator, the fundamental wave is assumed to cause the entire magnetic flux. All low frequency magnetic flux density measurements were done for all the measuring points A-H which were introduced in the previous chapters, these are presented in tables 7-10 in appendix A. These are meant to give information on whether the magnetic flux density stays below the safety limits and how does the screening and load changes affect the magnetic flux at low frequencies (10 Hz-2 kHz).

Measurements were taken from test cell 3, results from measuring points are presented in table 9 in appendix A. The highest measured value was 274 µT, which was measured under the power cabling at the point where cabling is turning to power cable ladders from

the generator. During the measurements, it became clear that the power cables are the source of the most severe low frequency H-fields, since even the highest magnetic flux densities measured straight from the generator frame were below 120 µT. These measurements indicate that instead of the generator, the cabling is acting as a primary source of low frequency H-fields.

Measurements were taken from the converter room. The highest magnetic flux density value 1011 µT was measured straight from the step-up transformer frame near the measuring point H. Since current THD of the converter should be less than 5 %, that means that minimum 95 % of low frequency H-field radiation is caused by 50 Hz current. Because H-field strength is proportional to current this same ratio can be applied for H-field strength and therefore also to the magnetic flux density. Minimum magnetic flux density caused by fundamental current is calculated in equation 9. As a result, a nominal 50 Hz frequency should generate H-field with flux density of at least 960 µT. Occupational health and safety requirements have set low AL at value of 1000 µT for 50 Hz H-field, the calculated value managed to stay just under the limit.

$$1.011\ mT \times 95\ \% = 960\ \mu T \quad (9)$$

The magnetic flux density was measured from the test area with synchronized generators. A test was done for the engine generator set introduced in chapter 5.4, where external magnetized generator was used as a load for the tested engine. A power cabling which was connected to generator's supply terminals gave highest magnetic flux density measurement. Values were highest when measuring device was set right between two phases. Measurements made between two phases are shown in figure 45. Figure 45 shows also the highest value measured 2002 µT, which is over twice the AL value set for 50 Hz H-field. These cables lay separately at the test area which is the reason for such high magnetic flux density. By tying these cables as a bundle, measured maximum magnetic flux density was reduced to a value of 606 µT, which is less than 1/3 of the value measured between two phases. This indicates that by proper routing H-fields will manage to stay below the AL values. The generator frame gave the maximum value of 18.4 µT, which is at such a low level that there is no concern that the generator itself will exceed the AL values. The test indicates that the power cabling is the source of most severe H-fields also in this situation. The biggest generators in the engine laboratory are in the same power

range, which makes these results applicable for assessing the exposures in the engine laboratory.

Figure 45. *Magnetic flux density measurements taken between two phases.*

MV circuits at the laboratory work with a relatively low 10,5 kV nominal voltage with the nominal frequency of 50 Hz. It is obvious that the strongest E-fields operate at this frequency. Devices for measuring E-field at frequencies below 9.5 kHz were not available and that is why only assumptions can be made for low frequency E-fields. The AL value for 50 Hz E-field can be calculated with the equation 10. It gives 10 kV/m for low AL value. The voltage of 10 kV can be considered low for medium voltage, since in Finland normally is used 20 kV in MV distribution systems. Because of this it would be logical to assume that 10 kV voltage at screened cable is not causing E-fields exceeding the AL values [28]. Since the capable measuring device was not available the verified results could not be done.

Static field measurements were not done since capable measuring devices were not available. All tests indicate that in the engine laboratory the source which creates most severe H-fields is the supply cabling coming from the generator, not the generator itself. Magnetic flux density measurements done to external magnetized generator show that the orientation of generator supply cables plays a major role in whether the magnetic flux density stays below the AL values. However, it is safe to assume that working in test cells should be safe in sense of magnetic fields, if the phases of supply cabling are not forming loops. This can be secured by tying cables to run close in parallel or tying them as a

bundle. Magnetic flux density values which were measured near the transformer were close to the AL values, which makes it recommended to simply block area near transformers to protect workers from getting exposed to H-fields. High frequency E-field measurements were all under the AL values. Measurement device for low frequency E-fields were not available, because of this assessment is the laboratory safe in sense of electric fields can not be done.

5. ACTIONS TO AVOID DISTURBANCES AND THE RESULTS

This chapter introduces solutions which are meant to reduce emission coupling based on the authors own ideas, literature and the protection basics presented earlier in chapters 2.5 and 2.6. These solutions are applied for test cell 3 and the emissions presented there. The solutions are assuming that the power cabling between the generator and converter is acting as a source of the emissions, which is based to measurements taken earlier. These solutions are meant either to prevent the emissions from propagating from the power cables or to block emissions from coupling with measurement circuits. At the end this chapter presents how implementation of screening solutions is affecting both induced disturbances and measured emissions.

5.1 Solutions to avoid coupling of the disturbances

This part introduces a few applicable solutions for the electromagnetic issues faced in test cell 3. In laterFF sections measurement results will be presented and conclusions will be drawn on the effectiveness of the proposed solutions.

Probably the easiest solution to reduce electromagnetic emissions from propagating to environment is to build conductive covers around the power cabling. The reason for this is that conductive screening blocks electromagnetic radiation like the faradays cage. However, this might cause overheating because airflow is essential for cooling of power cables and covers tend to block air flow near the cabling. To avoid this risk only steel bottom plates were installed under the power cables. This does not provide as good electromagnetic screening, but might be a perfect solution for this case since the signal cable ladders are running straight under the power cables. To get the most benefit from this solution, earthing should be done from both ends of the ladders. This way the screening should work against both E- and H-field propagation like it was described in chapter 2.5. Figure 46 presents the principle drawing of steel bottom plates manufactured by MEKA Pro Oy.

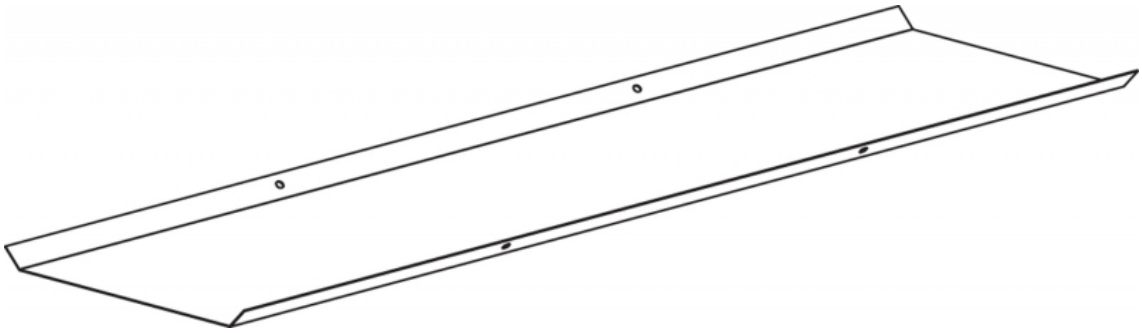

Figure 46. *A steel bottom plate for cable ladders [9].*

A solution which aims to prevent from emissions to couple with signal cables is to install these cables inside conductive conduits. Because measurement signals are not meant to transfer high currents, the risk of overheating should be low. In cases where cables are not running on the cable ladders the easiest way to do this is by using flexible metal conduits. In this case, a solid aluminium pipe works perfectly, since measured cables are running through the cable ladders. To ensure the protection against the H-field propagation these conduits must be connected from both ends to the earth potential, as was presented in chapter 2.5. Figure 47 presents five pieces of different size aluminium conduits.

Figure 47. *Five pieces of different size aluminium conduits [8].*

A solution that has already been applied in laboratory is to re-route the cables to get greater separation distance between the emission source and the victim of disturbances. Before the operation it is necessary to determine the source of emissions and the part of the victim circuit that is coupling with radiating emissions. After this, it is possible to re-route either the victim circuit or the source circuit to avoid the coupling of disturbances.

Disturbances can be attenuated if the frequencies of the most harmful disturbances are known. This can be done by installing an additional low pass filter to the measurement circuit before the measuring device or simply by using a measurement device with a lower cut off frequency. If additional low pass filtering is implemented, the filter should be designed so that does not reduce the measuring accuracy. In test cell 3, all measurements are indicating that the frequency range causing most harmful disturbances is above 50

kHz. By installing a low pass filter with a cut off frequency of 50 kHz to the measuring circuit should attenuate the disturbances from the measurements.

5.2 Screening efficiency of the aluminium conduit

Chapter 5.1 presented a few solutions for avoiding disturbances from coupling with signal conductors. This part introduces the screening performance of aluminium conduits. Aluminium conduits around the signal cables are not blocking the emissions radiating from the power cables, which is why it is unnecessary to do emission measurements with the spectrum analyser. Instead, these conduits will prevent from induction of electromagnetic disturbances to the signal cables. Disturbances induced after screening can be measured with an oscilloscope. The results are comparable with the oscilloscope measurements taken in chapter 4.1. By comparing these, conclusions can be drawn regarding how the conductive conduit works against the coupling of disturbances.

The setup of the oscilloscope measurement is exactly the same as the one used in earlier oscilloscope tests in chapter 4.1 to get comparable results. The oscilloscope measurement is shown in figure 48. All measurements can be found also in table 11 in appendix A. The measurements show that disturbance voltages are reduced after screening the cable with aluminium conduits. Based on the table 11, it seems that screening by aluminium conduits leaves only 1.32 mV normalized disturbance voltage when the generator is running on full load which means that disturbance voltage is reduced total by 84.9 % These measurements indicate that the screening by aluminium conduits is really working against the coupling of electromagnetic emissions.

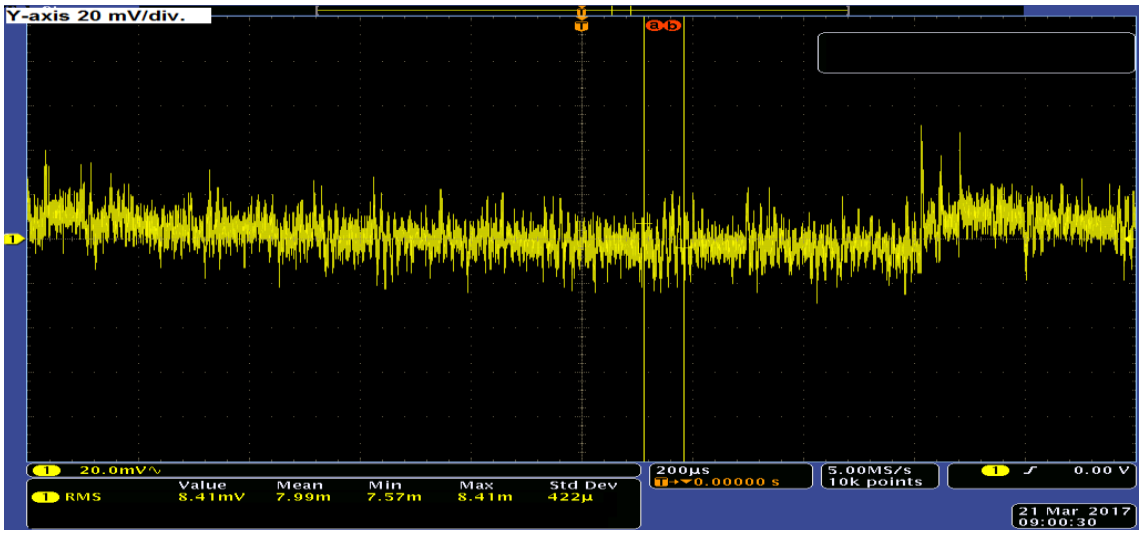

Figure 48. *A coaxial cable inside the aluminium conduit 100% load, 200 µs/div.*

5.3 Screening efficiency of the steel bottom plates

Earlier in this chapter the steel plates were introduced as a solution against the propagation of electromagnetic emissions from the power cables. In this subchapter steel bottom plates are installed under the power cables and their screening performance is evaluated. For comparison measurements are taken with a spectrum analyser, a magnetic field density meter and an oscilloscope.

The bottom plates were installed under the power cable ladders in test cell 3. Because of a limited amount of material, the bottom plate screening was built only for a length of 10 meters. Starting from the point where the cabling comes out from the generator and ending to where the platform ends. The steel bottom plates were installed only for two lower cable ladders. Figure 49 shows the bottom plate installation.

Figure 49. *The installed steel bottom plates.*

Screening performance was tested with the oscilloscope measurements. These measurements were done with exactly the same test setup as earlier measurements, the engine running with 100 % load which means that result should be comparable with the results taken earlier. Figure 50 shows measurement taken with steel bottom plates, measurement results are presented also in table 11 in appendix A. According to table 11, bottom plates block emissions in the same way as aluminium conduits did, since the bottom plate installation leaves only a 1.58 mV normalized disturbance voltage. This is an 81.9 % reduction compared to the situation where no additional screening was used.

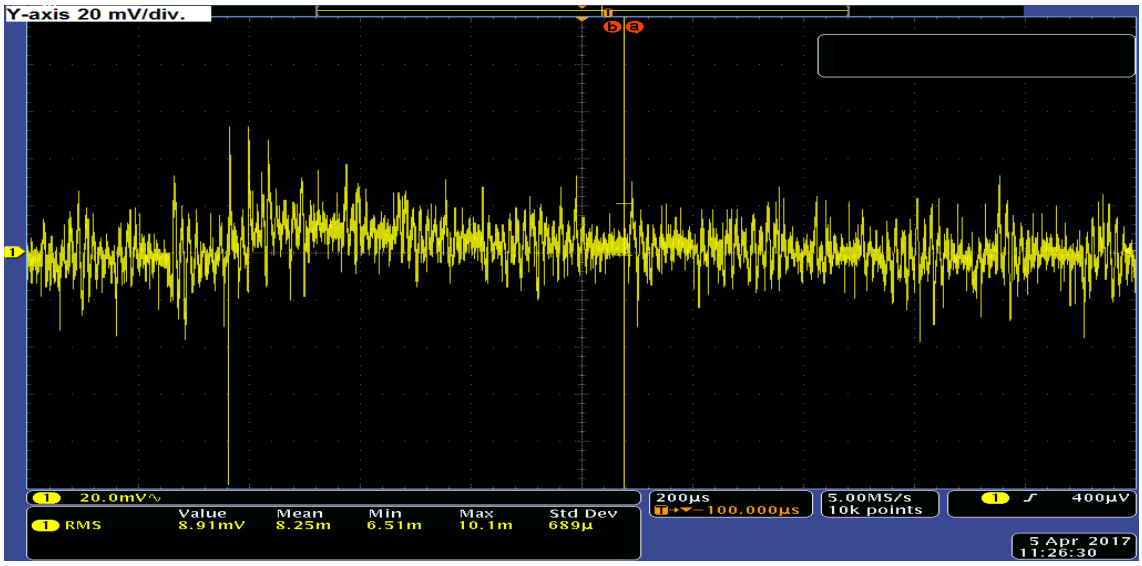

Figure 50. *The engine running with 100% load, steel bottom plates provided, 200 µs/div.*

The spectrum analyser measurements were taken from exactly the same measuring points in test cell 3, from which the measurements in chapter 4.2 were taken. The measurements were done with the generator supplying 100 % load to get comparable results to earlier measurements. Results are shown in table 10 in appendix A. Measuring points A & B are not valid for this comparison either, because external disturbances can have big influences to these measurements since measured values from these points were at such low level. The comparison between the unscreened and screened measurements is presented in table 6. Equation 14 presents how the difference to unscreened values is calculated. In the equation $V_{Screened}$ is the measured H- or E-field value when the engine is running with 100 % load and steel bottom plates are installed under the power cables. Value V_{100} is measured while the engine was running with 100 % load without additional screening provided for the power cabling. Equation 15 presents how change % values are calculated. In the equation $Diff.$ is difference value calculated in equation 14. All these results are shown in table 6. Based on table 6 it seems that screening have reduced the emissions measured at the signal cable ladders from the measuring points C and E. At these points both E- and H-field strengths are reduced more than 50 %. Measurements got from point D have not reduced, in fact they have risen after the screening. The reason for this is because of the bottom plates are not blocking emissions from the power cabling and the measuring point D is on the power cable ladders. This means that bottom plates should not even have any effect on the measurements taken from the point D.

$$Diff. = V_{Screen} - V_{100} \quad (14)$$

$$Change\ \% = \left(\frac{Diff.}{V_{100}}\right) \times 100 \quad (15)$$

Magnetic flux density measurements were done for getting information on how screening affects low frequency H-field propagation. These measurements were taken with the magnetic flux density meter from a measuring range of 10 Hz-2 kHz. During these measurements it became clear that screening reduces magnetic flux density at measuring points E and C which are located at signal cable ladders. According to chapter 2.5, screening with conductive materials should not generally significantly affect to propagation of low frequency H-fields. These measurements prove otherwise, since magnetic flux density is reduced more than 60 % at both measuring points C and E from the signal cable ladders.

According to these measurements, steel bottom plates block both high and low frequency H-fields and high frequency E-fields effectively. According to the theory, screening should work well against low frequency E-fields as well. These measurements were taken with earth connected only to one side of the cable ladders. Two earth connections on both ends of cable ladders might provide even better protection against electromagnetic radiation.

Table 6. *Screening performance of the steel bottom plates.*

Screening effects compared to values got before screening						
100% load	Electric field E		Magnetic field H		Magnetic flux density B	
Meas. Point	Diff. µV/m	Change %	Diff. µA/m	Change %	Diff. µT	Change %
C	-1054.6	-79 %	-8804.7	-57 %	-60.7	-65 %
D	1215.8	44 %	-1271.8	-7 %	40.4	76 %
E	-819.42	-75 %	-24421.7	-59 %	-46.45	-76 %

5.4 Screening efficiency of the steel bottom plates and the aluminium conduits combined

This part presents screening properties of both the aluminium conduits and the steel bottom plates. The combined screening performance of these can only be measured with the oscilloscope. This is done with the same setup the previous oscilloscope measurements were taken when the WDF engine was running with 100 % load on it.

The measuring results are presented in figure 51, and in table 11 in appendix A. The results show that the normalized disturbance voltage is reduced by just a few hundred micro volts more compared to the previous two screening actions separately. Table 11 shows that the normalized disturbance voltage is only a 0.93 mV, which is an 89.3 % less than the normalized disturbance voltage induced without additional screening. It also shows that the combined situation reduces the normalized disturbance voltage by a 0.39 mV compared to the situation where only aluminium conduits were used and by a 0.55 mV compared to situation where only steel plates were used. Based on these results, steel

bottom plates or aluminium conduits should provide separately sufficient screening compared to the situation where both are in use. The results indicate that if screened by using either one of these two methods, additional screening does not provide much of benefits in terms of blocking the unwanted disturbance voltages.

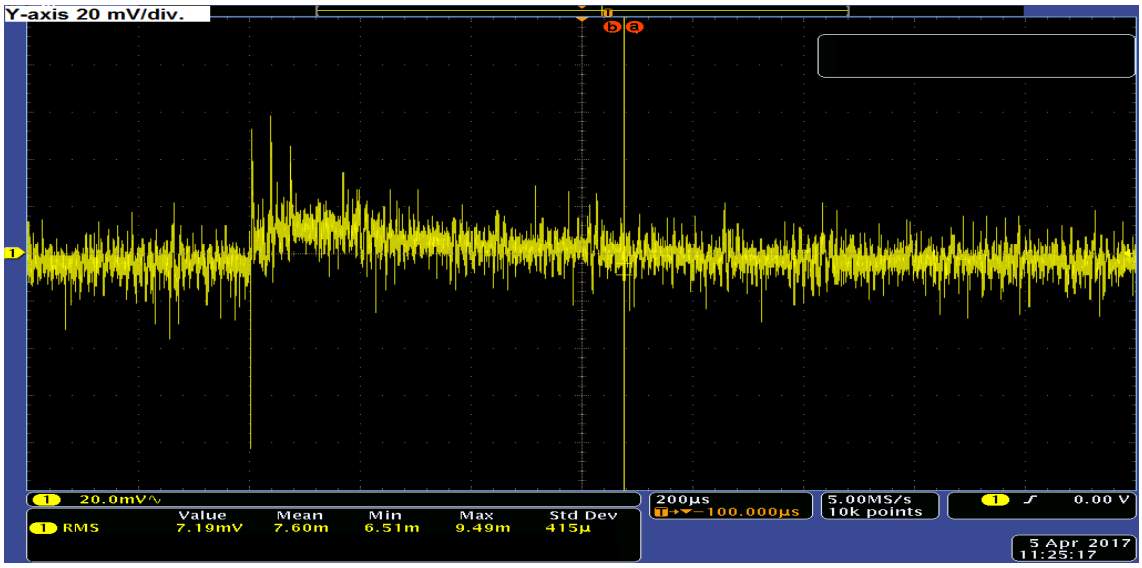

Figure 51. *The engine running with 100% load, steel bottom plates and aluminium conduits provided, 200 µs/div.*

6. CONCLUSIONS

The aim of this study was to find out what kind of electromagnetic emissions are present in the engine laboratory and how different actions are affecting to these emissions and the susceptibility of the measured system. Aim was also to verify whether the electromagnetic radiation stays below the limits set by Ministry of Social Affairs and Health.

To give the reader the understanding regarding electromagnetic fields and effects of variables to this phenomenon, the first part of the text introduced some of the most important principles related to electromagnetic fields and emission propagation formulas. It also introduced solutions for avoiding electromagnetic disturbances, and presented measuring devices that are used for electromagnetic measurements.

The study presented electromagnetic measurements taken from the engine laboratory, which were meant to give more information regarding the emissions present there. As a result, it became clear that generally power cabling is the source of most severe electromagnetic emissions. Based on the measurements and analysis made from engine laboratory it is safe to assume, that in general, test cells should be safe palaces to work in sense of the H-fields. Exception for this can be situations where supply cabling forms loops, since high currents running through loop can cause severe H-fields around it. To avoid H-fields generated from the cabling, cables should be spaced to run close in a parallel or tied as a bundle. These assumptions are done for the generators with a 10.5 kV supply voltage, which are run by engines with output power up to 8 MW. For ensuring the that the laboratory is not exceeding any of action levels, it would be recommended to do further studies regarding the E-fields and the static fields, which were not tested during this study. In the future, all the special applications such as power converters should be tested separately regarding occupational electromagnetic exposure limits.

This study introduced principles of how these emissions can be controlled, this was done by presenting a couple of applicable solutions to avoid high frequency disturbances. Two screening actions of these were applied at test cell 3 and the results were analysed. These solutions seemed to provide protection for the measurement signals, since the disturbance voltage measured with oscilloscope reduced by 70-80 %. The high frequency electromagnetic emissions were reduced by 79-57 % below the power cable ladders. Steel bottom plates gave protection also against low frequency H-fields. As a conclusion, this thesis provides knowledge for future issues related to electromagnetism, and gives knowledge how to avoid them.

REFERENCES:

[1] T. Williams, EMC for product designers, 4.th edition, Newnes 2011, 498 p.

[2] P.A, Chatterton, M.A. Houlden,– EMC Electromagnetic Theory to Practical Design, John Wiley & Sons 1996, 295p.

[3] Full Power Converter FPC-6000-4x25 technical specification, 2013, 23 p.

[4] L. Korpinen, Sähkömagneettisten kenttien terveysvaikutukset.[Cited:16.05.2017] Available: http://www.leenakorpinen.fi/?q=vaasa_egirls/opiskele_omatoimisesti/sahkomagneettiset_kentat/kentille_altistuminen/terveysvaikutukset

[5] T. Williams, K. Amstrong, - EMC for Systems and installations, Newnes 1999, 312p.

[6] IEC 60034-9 Rotating electrical machines, part 1: Rating and performance, International Electrotechnical Commission, 2010 12th. p.68, 139p.

[7] Instruction manual, Near field probe set – Model EHFP-30, Electro-metrics A Penril Corporation 1991, 4 p. 6 p.

[8] Alumiininen asennusputki JAP, ELWIA systems. [Cited:18.05.2017] Available: http://www.elwia.fi/fi/tuotteet/asennusputket-alumiini/asennusputket-alumiini-asennusputki/?tuote=alumiininen-asennusputki-jap

[9] POL Pohjalevy, MEKA Pro oy. [Cited: 07.01.2017] Available: http://www.meka.eu/tuotteet/tikashyllyt/suojakannet-ja-erotuslevyt/ks20/pol-pohjalevy.html.

[10] B. A Olshausen, Aliasing PSC 129 – Secondary processes. [Cited: 04.02.2017] 6 p. Available: http://redwood.berkeley.edu/bruno/npb261/aliasing.pdf

[11] H. De Groot, Danfoss webpage. [Cited:04.02.2017] Available: http://www.focusondrives.com/more-about-grounding-and-shielding/

[12] AVL Austria, Manual Indimodul 621 Product guide, 2005, AT1463E, Rev 02. p.66

[13] Frequency response of low pass filter. [Cited:23.2.2017] Available: http://www.angelfire.com/planet/funwithtransistors/Book_CHAP-2.html

[14] L. Puranen, Voimajohtojen terveysvaikutuksista ei ole täyttä varmuutta, STUK [Cited:1.3.2017] Avalilable: http://www.stuk.fi/aiheet/sahkonsiirto-ja-voimajohdot/voimajohtojen-terveysvaikutuksista-ei-ole-taytta-varmuutta

[15] Sosiaali- ja terveysministeriön asetus ionisoimattoman säteilyn väestölle aiheuttaman altistumisen rajoittamisesta. [Cited:1.3.2017] Available: http://www.finlex.fi/data/sdliite/liite/4354.pdf.

[16] The Switch, Permanent magnet generators. [Cited:23.03.2017] Available: http://theswitch.com/wind-power/permanent-magnet-generators/

[17] Valtioneuvoston asetus työntekijöiden suojelemiseksi sähkömagneettisista kentistä aiheutuvilta vaaroilta. [Cited:4.4.2016] Available: http://www.finlex.fi/fi/laki/alkup/2016/20160388

[18] Straight Talk About PWM AC Drive Harmonic Problems and Solutions. [Cited:8.3.2017] Available: https://www.ab.com/support/abdrives/documentation/techpapers/Harmonicsbasics.pdf.

[19] Real time spectrum analysers, what are they? [Cited:19.03.2017] Available: http://www.radio-electronics.com/articles/test-measurement/realtime-spectrum-analyzers---what-are-12.

[20] Hioki 3470 manual, Hioki E.E. Corporation, 2006, 9 p. 114 p.

[21] J. Sorila the representative of The Switch, Email. Received 21.02.2017.

[22] J. Puranen The big wind energy drive train technology debate. [Cited:29.03.2017] Available: http://www.renewableenergyworld.com/articles/2014/04/the-big-wind-energy-drive-train-technology-debate.html.

[23] H. Honkanen. Loisteho, yliaalot ja kompensointi. [Cited: 29.03.2017]. Available: http://gallia.kajak.fi/opmateriaalit/yleinen/ho-Har/ma/STEK_Loisteho,yliaallot%20ja%20kompensointi.pdf

[24] ICNIPR Guidelines for limiting exposure to time-varying electric and magnetic fields. [Cited:03.04.2017] Available:http://www.icnirp.org/cms/upload/publications/ICNIRPLFgdl.pdf.

[25] K. Jokela, A. Niittylä, Altistumisen rajoittaminen, STUK [Cited:03.04.2017] Available: https://www.stuk.fi/documents/12547/494524/6_8.pdf/51fdeebd-49c4-481b-8e26-5d4a7c903247

[26] Directive 2013/35/EU of European parliament and the council. [Cited:09.04.2017] Available: http://eur-lex.europa.eu/legal-content/EN/TXT/?uri=celex%3A32013L0035

[27] Total Harmonic Distortion and Effects in Electrical Power Systems [Cited:18.04.2017] Available: http://www.aptsources.com/resources/pdf/Total%20Harmonic%20Distortion.pdf

[28] L. Korpinen. Sähkön siirto ja jakeluverkot. [Cited: 08.04.2017] Available: http://www.leenakorpinen.fi/archive/svt_opus/3sahkon_siirto_ja_jakeluverkot.pdf

APPENDIX A: MEASUREMENT RESULTS

Table 7. *Measurements taken while the generator was standing still*

Peak values from measuring points				
Gen. standing still	Magnetic field H		Electric field E	Magnetic field density B
Measuring point:	dbµA/m	µA/m	µV/m	µT / range 10Hz-2kHz
A	33.2	45.7	20.3	0.045
B	35.6	60.3	14.1	0.042
C	26.7	21.6	24.7	0.050
D	26.8	21.9	33.7	0.038
E	26.4	20.9	38.0	0.057

Table 8. *Measurements taken while the engine was running with 0 % load*

Peak values from measuring points				
0% load	Magnetic field H		Electric field E	Magnetic field density B
Measuring point:	dbµA/m		µV/m	µT / range 10Hz-2kHz
A	50.6	339	31.3	3.8
B	71.4	3715	71.3	4.2
C	80.5	10593	779.3	1.2
D	82.5	13335	2990.3	4.4
E	87.4	23442	821.7	4.9

Table 9. *Measurements taken while the engine was running with 100 % load*

Peak values from measuring points before additional screening				
100% load	Magnetic field H		Electric field E	Magnetic field density B
measuring point:	dbµA/m	µA/m	µV/m	µT / range 10Hz-2kHz
A	57.6	759	23.2	12.8
B	73.0	4467	62.7	24.3
C	83.8	15488	1343	92.7
D	85.6	19055	2788	53.2
E	92.3	41210	1096	61.0
F	93.3	46238	3736	93.7
G	78.4	8318	106	255.0
H	23.6	15.1	73.8	1011*
*Value is measured near the transformer frame, not from the same point that other measurements were taken				

Table 10. *Meas. taken while the engine was run. with 100% load, bottom plates inst.*

Peak values from measuring points after screening				
100% load	Magnetic field H		Electric field E	Magnetic field density B
Measuring point:	dbµA/m	µA/m	µV/m	µT / range 10Hz-2kHz
A	67.0	2239	72.4	12.8
B	67.0	2239	77.8	24.3
C	76.5	6683	288	32.0
D	85.0	17783	4004	93.6
E	84.5	16788	276	14.6

Table 11. *Oscilloscope measurements*

Oscilloscope measurements					
	Meas. value	Dist. Volt. originating from the power cabling**		Reduction to reference*	
Screening:	VRMS mV	VRMS mV	%	VRMS mV	%
Without additional screening 100% load (ref)*	15.40	8.73	100%	0.00	0
Without additional screening 0% load	13.1	6.43	74%	0.00	0%
Aluminium conduit 100 % load	7.99	1.32	15%	-7.41	-84.9 %
Steel bottom plates 100% load	8.25	1.58	18%	-7.15	-81.9 %
Aluminium conduit & steel bottom plates 100 %	7.60	0.93	11%	-7.80	-89.3 %
Permanent magnet generator standing still	6.67	0.00	0%		
*The 100% load without additional screening measurement is used as a reference on 100% load comparions					
**Normalized disturbance voltage = Meas. RMS value - Meas. RMS value with permanent magnet generator standing still					